Contents

Precision Tests of Electroweak Physics: Current Status and Prospects for the Next Two Decades

Frank S. Merritt

University of Chicago, Chicago, IL 60637

Hugh Montgomery

Fermi National Accelerator Laboratory, Batavia, IL 60510

Alberto Sirlin

New York University, New York, NY 10003

Morris Swartz

Stanford Linear Accelerator Laboratory, Stanford, California 94309

1 Introduction

We present a brief review of the present status and prospects for progress in electroweak measurements leading to precision tests of the Standard-Model Electroweak Theory. Our emphasis is on the measurements of electroweak couplings, of the masses of the W and Z gauge bosons, and of the searches for and mass measurements of the top quark and the Higgs boson.

Section 2 contains a brief review of the standard theory, and Section 3 summarizes the schedule of the major experimental programs expected to run during the next 15 years. Sections 4 and 5 cover measurements of electroweak couplings at high and low q^2, respectively. Section 6 is devoted to precision measurements of the W mass at Fermilab and LEP 2. Section 7 describes the status of the top quark searches at Fermilab, and the anticipated future improvements in direct top mass measurement. Section 8 describes the electroweak fits of all of these data to the Standard Model. For the first time, these measurements are beginning to give significant constraints on the Higgs mass. The precision of the Standard-Model predictions of the Higgs mass based on indirect measurements provides a useful benchmark for evaluating the experimental program. We have attempted to project how the resolution of these predictions will evolve over the next 15 years, and to see where significant improvements might be made. The ultimate test of the Standard Electroweak Theory may lie in the comparison of these indirect determinations of the Higgs mass with its direct observation. In Section 9 we review the direct searches for the Higgs anticipated in future years. The measurement of triboson couplings is briefly discussed in Section 10. A summary and conclusions are presented in Section 11.

We have drawn heavily on the work of others, particularly in workshop proceedings, design reports, and summary talks. The field of precision electroweak measurements is evolving rapidly, both in terms of new measurements from Fermilab, CERN, and SLAC, and also in terms of new studies relating to future experiments and facilities. We have attempted to include new information as it has become available, but it is clear that new developments will continue to emerge over the next few months in several important areas. These include:

- final measurements of M_W from Run 1a data from both CDF and DØ,
- improved estimations of LHC detector performance (from ATLAS and CMS TDR's),
- improved projections of LEP 2 energy and schedule, based on continuing RF studies,
- better estimates of ultimate LEP 1 errors and running plans for 1995, and
- better understanding of theoretical and experimental limitations in determining $\alpha(M_Z)$.

2 Standard Electroweak Model.

This section is based on a more extensive overview [1] prepared for this working group.

2.1 Overview

Because of its success in describing low energy phenomenology and its relative economy in the number of fundamental fields, the $\mathrm{SU}(3)_c \times \mathrm{SU}(2)_L \times \mathrm{U}(1)$ theory of

strong and electroweak interactions, based on the principle of non-abelian gauge invariance, has become the Standard Model (SM). $SU(3)_c$ embodies the current theory of the strong interactions, Quantum Chromodynamics, and is deemed to be an unbroken symmetry of nature. The $SU(2)_L \times U(1)$ sector is the basis of the Standard Electroweak Model and is spontaneously broken at a mass scale $v = (\sqrt{2}G_\mu)^{-1/2} = 246$ GeV[a] into $U(1)_Q$, the abelian gauge group of electromagnetism. The theory is endowed with the fundamental properties of renormalization and asymptotic freedom of the strong interactions. The minimal version involves three generations of quarks and leptons and one Higgs doublet.

The SM has been very successful phenomenologically. It has provided the theoretical framework for the description of a very rich phenomenology spanning a wide range of energies, from the atomic scale up to M_Z. It is being tested at the level of a few tenths of a percent, both at very low energies (superallowed Fermi transitions, low energy decays) and at high energies (CERN, Fermilab, SLC). The aim of these studies is to test the theory at the level of its quantum corrections and to search for deviations that may signal the presence of "new physics".

There are two basic missing pieces in the SM: the top quark and the Higgs boson. Very suggestive, but not definitive, evidence for the existence of the top quark with a mass $M_t = (174 \pm 10^{+13}_{-12})$ GeV has recently been presented [2] by the CDF experiment. There are compelling theoretical reasons for believing that the top quark exists:

- It is known [3] that the left-handed b has quantum numbers corresponding to the lower component of an isodoublet and, therefore, its partner must exist; and
- The top quark is necessary to complete the cancellation of anomalies, a basic requirement for renormalizability [4].

The analysis of the precision electroweak data leads at present to the prediction that M_t lies in the vicinity of 175±30 GeV, as discussed in Section 8; this constraint arises from the top quark contribution to the electroweak radiative corrections.

The most fundamental discovery to be made in the framework of the SM would be the detection of the Higgs boson or, more generally, the elucidation of the Higgs sector of the theory. In fact, this may lead us to understand the nature of electroweak symmetry breaking and the generation of mass. Perturbative partial wave unitarity [5] in the $J = 0$, $I = 0$ channel for $W_L^+W_L^- \to W_L^+W_L^-$ requires $|5\lambda/16\pi| < 1/2$, where λ is the quartic Higgs coupling. Using $M_H^2 = 2\lambda v^2$, this implies $M_H \leq 780$ GeV. This roughly represents the mass scale at which the Higgs sector becomes strongly interacting. For larger values of M_H, the unitarization of the S-matrix requires some manifestations of "new physics" and one expects the formation of resonances such as ρ-like vector mesons. There is also an interesting lower bound from the requirement that the SM vacuum be stable [6]:

$$M_H(\text{GeV}) \quad > \quad \begin{array}{l} 136.3 + 2.2(M_t - 174) \\ -\frac{4.5}{0.007}(\alpha_S(M_Z) - 0.118) \end{array} \qquad (1)$$

This bound assumes that the SM is valid up to mass scales $\simeq 10^{15} - 10^{19}$ GeV.

There are strong arguments to expect that, sooner or later, "new physics" will be revealed. The SM contains a plethora of adjustable parameters, most of them associated with the mass matrices of the matter fields, leptons and quarks. If the neutrinos are massless, we have three gauge couplings, M_Z, M_H, three lepton masses, six quark masses, three mixing angles and one CP-violating phase in the CKM matrix, and one CP and P violating Θ parameter, a total of 19 constants (we assume that the Planck mass $M_P \simeq 1.2 \times 10^{19}$ GeV defines the unit of mass). If the neutrinos have mass there are seven additional parameters. The SM also fails to provide a reason for the observed quantization of electric charge and the number of generations. Particularly suspect is the mechanism of symmetry breaking involving a single Higgs doublet. As the self-energies of the scalar fields are quadratically divergent, one has $M_H^2 = M_{0H}^2 - c_\lambda \Lambda^2$, where M_{0H} is the bare mass, Λ is the ultraviolet cutoff, and c_λ is a constant of $\mathcal{O}(\lambda)$. If one assumes that a natural cutoff will emerge at the Planck mass, we have $\Lambda \approx M_p$, and this means that M_{0H} must be fine-tuned to an unnatural precision to maintain M_H at the v scale. The same hierarchy problem emerges if one embeds the SM in a GUT involving scales $\Lambda \gg M_H$. Two main schools of thought have emerged to circumvent this problem. One approach is dynamical symmetry breaking via fermion-antifermion condensation, $\langle \bar{\psi}_R \psi_L + h.c \rangle \neq 0$. Examples include technicolor [7] and $t\bar{t}$ condensation models [8]. The fact that the top quark is the only fundamental fermion with $M \sim v$ may be a strong indication that it is involved in the mechanism of symmetry breaking. Another scenario is supersymmetry. Here Higgs scalars occur as fundamental fields, but the quadratically divergent contributions to their self-energies are cancelled by the fermionic counterparts. The minimal supersymmetric extension of the SM (MSSM) [9] involves two Higgs doublets. There are five Higgs bosons (two neutral scalars, 1 neutral pseudoscalar, and 2 charged) plus a rich spectrum of supersymmetric partners. The lighter Higgs boson satisfies the important constraint $M_H \lesssim 130$ GeV. Recently, the SUSY approach has received support from the observation, derived from the precision electroweak analysis, that in the framework of the MSSM the three gauge couplings unify [10] at energies $\sim 10^{16}$ GeV.

[a] We choose units such that $c = 1$, and consequently masses are expressed in GeV rather than GeV/c^2 throughout this report.

2.2 *Input Parameters*

There are three accurately determined physical parameters [11] that play an important role as inputs in electroweak physics:

1. The fine-structure constant, measured most precisely from $(g\text{-}2)_e$, is

$$\alpha = 1/137.03599\ldots \quad (\delta\alpha/\alpha = 0.045 \text{ ppm}). \quad (2)$$

2. The muon decay constant G_μ, which may be regarded as the modern definition of the Fermi constant. It is determined, by definition, from the muon lifetime, by applying the radiative corrections of the local V-A theory, which in this case are convergent. The current value is

$$G_\mu = 1.16639(1) \times 10^{-5} \text{ GeV}^{-2} \quad (8.5 \text{ ppm}). \quad (3)$$

3. The Z mass, determined from the 1993 LEP data, is

$$M_Z = 91.1888 \pm 0.0044 \text{ GeV} \quad (48 \text{ ppm}). \quad (4)$$

For a long time it has been known that large radiative corrections, associated with the running of α, play an important role in electroweak physics. In particular, $\alpha(M_Z)$ is of special interest. This concept is scheme-dependent. A frequently employed definition is $\alpha(M_Z) = \alpha/(1-\Delta\alpha)$, where $\Delta\alpha$ is the fermionic contribution to the conventionally renormalized vacuum polarization function of QED, evaluated at $q^2 = {M_Z}^2$. We discuss the determination of $\Delta\alpha(M_Z)$ in a later subsection.

2.3 *Basic Radiative Corrections*

Knowing α, G_μ, M_Z, one can evaluate M_W and $\sin^2\theta_W$. At the tree level, this can be done from the basic natural relations:

$$M_W = M_Z \cos\theta_W, \quad (5)$$

$$e = g \sin\theta_W, \quad (6)$$

$$G_\mu/\sqrt{2} = g^2/8M_W^2, \quad (7)$$

where e is the positron charge and the weak mixing angle θ_W is given by $\tan\theta_W = g'/g$ (g and g' are the gauge couplings of $SU(2)_L$ and U(1), respectively). Equation (4) holds if additional doublets and singlets of Higgs scalars are introduced in the theory, but it is not generally valid for other representations, such as triplets. In order to carry out the analysis in the presence of radiative corrections, it is necessary to specify the precise definition of the parameters involved. It is convenient to identify M_W with the physical or pole mass, in analogy with M_Z. Regarding the weak mixing angle θ_W, a number of possibilities have been employed in the literature. Defining $\sin^2\theta_W = 1 - M_W^2/M_Z^2$, one finds [12]

$$s^2 c^2 = \frac{A^2}{M_Z^2(1-\Delta r)}, \quad (8)$$

where s^2 and c^2 are abbreviations for $\sin^2\theta_W$ and $\cos^2\theta_W$, $A^2 = \pi\alpha/(\sqrt{2}G_\mu) = (37.2802\,\text{GeV})^2$ and Δr is the radiative correction. Another possibility is to identify the weak mixing angle with the $\overline{MS}$ parameter $\sin^2\hat{\theta}_W(M_Z)$, evaluated at the M_Z scale. In this case one obtains [13]

$$\hat{s}^2\hat{c}^2 = \frac{A^2}{M_Z^2(1-\Delta\hat{r})}. \quad (9)$$

The quantities Δr and $\Delta\hat{r}$ are basic corrections of the electroweak theory. In particular, the definition of $\sin^2\theta_W$ and Eq. (6) imply that Δr is a physical observable, like g-2, for example. The parameter $\hat{s}^2$ is very convenient to describe physics at the Z peak and can be obtained almost directly from the on-resonance asymmetries with the application of very small radiative corrections. It is crucial for GUTs studies. The two most frequently employed renormalization methods lead precisely to the above definitions. The on-shell approach [12], which employs physical observables as renormalized parameters, leads in a natural manner to $\sin^2\theta_W = 1 - M_W^2/M_Z^2$. In the $\overline{MS}$ method [13], the counterterms are chosen to cancel the pole terms of dimensional regularization.

The dominant contributions to Δr and $\Delta\hat{r}$ arise from fermion loops and involve large logarithms of the form $\ln(M_Z/M_f)$, that can be associated with the running of α (M_f represents a generic fermion mass), and contributions from the t-b isodoublet which are very sensitive to M_t. There are also conceptually very important bosonic electroweak corrections involving virtual $W^\pm$, Z, γ and H. They affect self-energies, vertex and box diagrams but, in four fermion processes, they are numerically smaller than their fermionic counterparts. The leading asymptotic behaviors for large M_t and M_H are quadratic in M_t and logarithmic in M_H. They have opposite signs in both Δr and $\Delta\hat{r}$, which partially accounts for the fact that, in global analyses of the electroweak data, small (large) M_H values favor relatively small (large) values of M_t. The terms proportional to M_t^2 are analogous to those occurring in the fermionic correction [14]

$$(\Delta\rho)_f = \frac{3G_\mu m_t^2}{\sqrt{2}\,8\pi^2} \quad (10)$$

to the ρ-parameter, defined as the ratio of effective neutral to charged-current couplings at $q^2 = 0$. Because of an additional factor c^2/s^2 multiplying the M_t^2 contributions, Δr is much more sensitive to M_t than $\Delta\hat{r}$ or

$\Delta\rho$. Aside from Δr, $\Delta\hat{r}$, and $\Delta\rho$, other important radiative corrections include the electroweak form factor [15] $k(q^2)((k'(q^2))$ that multiplies $s^2(\hat{s}^2)$ in neutral current amplitudes, and the vertex correction to $Z \to b\bar{b}$ which exhibits an intrinsic M_t^2 dependence.

Complete one-loop calculations for various processes have been carried out by several groups. Although full two-loop calculations do not yet exist, leading contributions of $\mathcal{O}(\alpha^n \ln^n(M_Z/M_f))$, $\mathcal{O}(\alpha^2 \ln(M_Z/M_f))$ [12], $\mathcal{O}(\alpha^2(M_t^2/M_W^2)^2)$ [16], and $\mathcal{O}(\alpha\alpha_s, \alpha\alpha_s^2)$ are incorporated. The latter affect mainly the terms proportional to M_t^2 in $\Delta\rho$ [17] and in the $Z \to b + \bar{b}$ vertex [18], and depend sensitively on how M_t is defined. In current analyses one employs the pole-mass as this seems to be the parameter that can most readily be identified with kinematic measurements of M_t.

There is another definition of the weak mixing angle, $\sin^2\theta_W^{\rm eff}$ (also called $\sin^2\theta_{\rm eff}^{\rm lept}$), which is employed in the LEP analysis. Calling g_{V_ℓ} and g_{A_ℓ} the effective vector and axial vector couplings in $Z \to \ell\bar{\ell}$ at resonance (g_{V_ℓ} and g_{A_ℓ} absorb vertex and self-energy corrections), one defines $1 - 4\sin^2\theta_W^{\rm eff} = {\rm Re}\, g_{V_\ell}/g_{A_\ell}$. It has recently been found [19] that $\hat{s}^2 = \sin^2\theta_W^{\rm eff} - 0.0003$.

The on-shell and $\overline{MS}$ schemes have been systematically applied to a number of fundamental observables, spanning $0 \le |q^2| \le M_Z^2$: atomic parity violation, νl scattering, $\nu_\mu N$ deep inelastic scattering and the various asymmetries, widths, and cross sections measured at LEP and SLC.

2.4 Evidence for Quantum Corrections

It has been known for at least two decades that radiative corrections play an important role in the analysis of the SM. For example, if only the Fermi-Coulomb function were included in the analysis of the superallowed Fermi transitions (as in ^{14}O decay), there would be a large violation of the unitarity of the CKM matrix and the SM would be placed in severe jeopardy. Fortunately, there are large corrections in semileptonic decays which literally rescue the theory from obvious contradiction. Furthermore, these corrections are divergent in the local V-A theory. Thus, the renormalizability of the SM and the fact that the resulting corrections are of the correct sign and order of magnitude play a crucial role in the tenability of the new theory [20].

In high-energy phenomena, the dominant radiative corrections involve virtual fermions. They are responsible for the large logarithms that can be absorbed in the running of α, and the contributions of the tb isodoublet, from which the M_t constraints are derived. One way to quantify this question is to "measure" $(\Delta r)_{\rm res}$, the residual part of Δr after extracting the corrections contained in $\alpha(M_Z)$. We have

$$\frac{\alpha}{1-\Delta r} = \frac{\alpha(M_Z)}{(1-(\Delta r)_{\rm res})}. \qquad (11)$$

Inserting the direct collider determination of $M_W = 80.23 \pm 0.18$ GeV in Equation 6, one finds $\Delta r = 0.0442 \pm 0.0104$. Using $(\alpha(M_Z))^{-1} \approx 128.84$, we have $(\Delta r)_{\rm res} = -0.0165 \pm 0.0111$. This differs from 0 by only $\approx 1.4\sigma$. Thus, if one employs only the direct M_W measurement, the evidence for $(\Delta r)_{\rm res} \neq 0$ is rather weak. The determination of Δr and $(\Delta r)_{\rm res}$ becomes much sharper if one employs all the direct and indirect information obtained by fitting the data to the full SM, with its plethora of radiative corrections and interlocking relations. In that case one currently obtains $M_W = 80.31 \pm 0.07 \pm 0.01$ GeV. Choosing $M_W = 80.32 \pm 0.07$ GeV (which corresponds to $M_H = 60$ GeV, the most unfavorable case) one finds $\Delta r = 0.0390 \pm 0.0041$ and $(\Delta r)_{\rm res} = -0.0221 \pm 0.0044$, which now differs from zero by 5σ!

Another interesting question is whether there is at present evidence in the high-energy observables for the conceptually important bosonic electroweak corrections, mediated by virtual $W^\pm$, γ, Z, and H. It has been recently shown [21] that two different determinations of $\sin^2\hat{\theta}_W(M_Z)$, namely from the on-resonance asymmetries and from Eq. (7), differ sharply if these corrections are subtracted and the complete fermionic corrections retained. The difference is 4σ for $M_t = 131$ GeV and reaches 7σ for $M_t = 180$ GeV. Thus, this simple argument gives strong evidence for the contribution of bosonic electroweak corrections in the SM.

2.5 S, T, and U Parameters

"New physics," *i.e.*, physics beyond the SM, may affect the quantum corrections. If the new physics is associated with a high-mass scale and affects mainly the self-energies, the idea has been proposed to parametrize its contributions in terms of three amplitudes [22] S_W, S_Z, and T. If the mass scale is much larger than M_Z, $(\alpha/4\hat{s}^2)S_W$ and $(\alpha/4\hat{s}^2\hat{c}^2)S_Z$ are essentially the contributions of the new physics to the W and Z wave function renormalizations, respectively, while αT represents the corresponding contributions to $\Delta\rho$. Alternatively, one defines $S = S_Z$, $U = S_W - S_Z$. T and U are primarily sensitive to the isodoublet mass splittings (generally, $U \ll T$), while S probes contributions from degenerate $SU(2)_L$ doublets. If a direct measurement of M_t is not available, the usual procedure is to evaluate the radiative corrections of the SM at standard values of M_t and M_H and fit S, T, and U from the data. In that case S, T, and U parametrize both effects of unknown particles, as well as departures of M_t and M_H from the standard values. In more recent discussions, it has become useful to introduce a fourth parameter, δ_b, that describes the departure

of the $Z_0 \to b\bar{b}$ width from the SM evaluation [23]. If a directly measured value of M_t is employed, it is sufficient to specify M_H. As the dependence of the radiative corrections on M_H is mild, it can be treated as part of the theoretical error. In this case S, T, U, and δ_b represent just the contributions from new physics. A very recent global analysis [24] that incorporates the CDF M_t value and the 1993 LEP data, gives

$$\begin{aligned} \mathrm{S} &= -0.15 \pm 0.25\ {}^{-0.08}_{+0.17} \\ \mathrm{T} &= -0.08 \pm 0.32\ {}^{+0.18}_{-0.11} \\ \mathrm{U} &= -0.56 \pm 0.61 \\ \delta_b &= 0.031 \pm 0.014. \end{aligned} \tag{12}$$

Except for δ_b (a $\sim$2 σ deviation), there are no indications of departures from the SM. An alternative formulation involves the ϵ_i(i=1,2,3,b) parameters [25], defined in terms of the physical observables M_W, , $_l$, $A_{FB}^{(l)}$ and , $_{b\bar{b}}$. It is worthwhile to note that S_W, S_Z, and T are actually parts of Δr and $\Delta\hat{r}$, which also include vertex and box diagrams in a gauge invariant manner. Therefore, instead of S_W, S_Z, and T, one can also employ $\Delta r = (\Delta r)_{SM} + (\Delta r)_{new}$, $\Delta\hat{r} = (\Delta\hat{r})_{SM} + (\Delta\hat{r})_{new}$, together with effective parameters $G_\mu(1+\hat{\alpha}T)$ and δ_b linked to the Z widths.

Since the early determinations, the data have favored $S < 0$. On the other hand, a fourth generation of degenerate chiral fermions gives $S \simeq 4/6\pi = 0.21$, while technicolor models roughly contribute $S \simeq (0.05 - 0.10)N_T N_D + 0.12$, where N_T and N_D are the number of technicolors and technidoublets, respectively (the 0.12 arises from a heavy effective Higgs scalar in the TC framework [26]). For one generation with $N_T = N_D = 4$, this leads to $S \simeq 0.9$ to 1.7. Thus, the current precision measurements disfavor the most typical technicolor models. On the other hand, supersymmetric theories don't introduce additional chiral fermions and tend to give very small S values. More generally, in the MSSM, the additional radiative corrections are small provided that the supersymmetric partners are much heavier than M_Z. In that limit, the radiative corrections become those of the SM with a light Higgs, $M_H \leq 130$ GeV [27]. Even if the supersymmetric partners are not regarded as very heavy, the decoupling limit provides a bound for the MSSM predictions.

2.6 Determination of $\alpha(M_Z)$

The renormalization of the electromagnetic coupling constant α to its value, $\alpha(M_Z)$, at the mass of the Z is a necessary step in the evaluation of many electroweak quantities. The theoretical error in the calculation is small [28,29] so that the error arising from the loops containing the leptons is small.

Table 1: Hadronic contributions to the determination of $\Delta\alpha$ and their errors.

Region	Contribution	Uncertainty
Resonances	0.00556	0.00018
Continuum 1.0 - 2.3 GeV	0.00198	0.00039
Continuum 2.3 - 9.0 GeV	0.00721	0.00072
Continuum 9.0 - 12.0 GeV	0.00169	0.00017
Continuum 12.0 - ∞ GeV	0.01237	0.00037
Total	0.0288	0.0009

In principle an analogous calculation of the relevant loops could be performed for the quarks, u, d, s, c, and b; however, the masses of the quarks are ill defined quantities. The usual approach is to express the calculation in terms of a dispersion integral over the electron-positron annihilation cross section into hadrons (scaled to that into muons). This ratio is often called R. The procedures used to make this evaluation have been discussed extensively [30,31]. The integral is evaluated in two parts, the resonances are parametrized and evaluated separately from the continuum regions. The contributions and the errors for the different regions are summarized in Table 1. The change in α, including leptonic contributions, is $\Delta\alpha = 0.0595 \pm 0.0009$ [31], and leads to $(\alpha(M_Z))^{-1} = 128.84 \pm 0.10$. The uncertainty is almost entirely due to the hadronic contributions listed in the table.

There are several experiments which might address individual resonance regions; for example there is a program at Novosibirsk [32] which will address the region from the ρ and ω to above the ϕ. New results are expected soon. The Daphne storage rings at Frascati will also operate at the ϕ resonance. However, the biggest individual contribution to the error comes from the region between 2.3 and 9.0 GeV, between charm and bottom thresholds. The data were taken from a single experiment and a systematic error assigned [31] to take account of differences between the results of that experiment and others for other measurements than R.

A reanalysis of existing data has recently been carried out (motivated by this DPF review) which has produced a result [33] differing from the old one by about two sigma. We have used the old value for all results in this paper in order to be consistent with other studies and with the currently accepted value. But this new result and similar work [34] underscore the importance of further theoretical and experimental studies directed toward improving the determination $\Delta\alpha$. Without this, in a few years the uncertainty in $\Delta\alpha$ will be one of the most limiting factors in improving the precision of the determination of the mass of the Higgs from indirect measure-

ments, as we show in Section 8.6 below.

3 Expected Schedule of Future Measurements

In this section we will briefly review the schedule and status of the experimental programs which are most important for precision electroweak measurements. The experimental measurements will be discussed in the following sections, and the combined electroweak tests are discussed in Section 8.

3.1 LEP and SLC

LEP has been running near the Z since 1989. The run of 1995 is scheduled to be the last year of LEP 1 data taking. Final integrated statistics are expected to be improved by perhaps a factor of 3 over that of most current analyses (based on data taken through the end of 1993).

With the installation of new superconducting RF cavities after the 1995 run, the LEP energy will be raised by about a factor of 2 and LEP 2 will begin data-taking in 1996. It is now expected that the LEP 2 energy will be 180 GeV. This is based on studies with the first superconducting cavities and allowing, as a safety margin, for up to 3 non-operating klystrons. LEP 2 will run for a minimum of three or four years, with the goal of attaining an integrated luminosity of 500 pb^{-1}. The most important physics goals for electroweak studies are the precision measurement of M_W and the extension of the Higgs boson search to higher masses.

It is technically possible to increase the LEP 2 E_{cm} by about 15 GeV by producing more superconducting rf cavities at a cost of about 130 MSF. This decision must be made by summer of 1995.

SLC has been running for two years using polarized beams, which allow the measurement of A_{LR}, and has accumulated about 50K events. Beam polarization has now been improved from 63% to 80%. It is expected that polarized running will continue for at least three more years, reaching a total of at least 500K events.

3.2 Fermilab

The Fermilab collider has completed Run 1a (25 pb^{-1}) and is now taking data in Run 1b. This is expected to last through 1995 and to accumulate at least 100 pb^{-1}. The run is going very well now with record luminosities being achieved; Run 1b may well exceed 150 pb^{-1} if this continues, but in this report we will continue to assume 100 pb^{-1}.

The fixed target run will begin in 1996 and will last for approximately one and a half years, producing an improved measurement of $\sin^2\theta_W$ from the deep-inelastic neutrino experiment E815. During this time, extensive upgrades of both the collider detectors and of the accelerator will be carried out. The Main Injector, which is crucial for high-luminosity collider running, should be completed in 1998.

In 1998 or 1999, Tevatron Run 2 will begin with the Main Injector and with upgraded collider detectors. This run will provide about a factor of 5 improvement in luminosity, and is expected to accumulate at least 1000 pb^{-1} of data within two or three years.

It should be noted that all of the direct information about the top quark obtained over the next decade will come from the Fermilab collider program. This is a crucial part of electroweak physics. Improvements in statistics in both Run 1b and Run 2 could give significant improvements in measurements of M_t and M_W, and consequent improvements in electroweak tests.

3.3 LHC

This accelerator is expected[b] to begin operation in about the year 2004, using the existing LEP tunnel with high-field magnets to collide pp beams at $E_{cm} = 14$ TeV. The CERN Council formally approved the project in December 1994. Two experiments, ATLAS and CMS, have been given first-stage approval and their collaborations are completing design reports which will be submitted later this year. Extensive studies of LHC physics and detector design have been carried out and presented in the "Letters of Intent" of these experiments.

The LHC is essential for improved electroweak tests in several important areas. For precision electroweak tests, it should provide the best measurement of the top mass and extensive information about top production and decays, and will improve the precision of measurements of triboson couplings. Most importantly, it will extend the search for the Higgs boson over the mass region 80-800 GeV, which may provide the ultimate test of the electroweak theory.

3.4 Other Possibilities

There have been extensive studies [35,36] of the potential for an e^+e^- linear collider with energy $E_{cm} \geq$500 GeV (the "Next Linear Collider", or NLC). In several sections of this report we make allusions to some of this potential. However we have not considered the time frame associated with such a collider to be the primary subject of this report. The treatment of the NLC is therefore not to be

[b] The CERN Council voted unanimously to approve the LHC on December 16, 1994, after this report had been completed. Because of financial consideration, the approval requires staging of the project unless there is significant financial participation by non-member states, and especially by the United States. In this report, we have only considered the machine parameters and schedule that were originally proposed, which we hope in the end will turn out to be the correct ones.

considered complete. For further discussion, see also the reports of the Electroweak Symmetry Breaking and the Accelerator subgroups of this DPF study.

During the past year there have been discussions of possible upgrades to the Tevatron Collider complex at Fermilab. These include a luminosity upgrade to $L = 10^{33}$ cm^{-2}sec^{-1} (TeV*) and a combined luminosity and energy upgrade (to $E_{cm} = 4$ TeV). Such possibilities are discussed by the Accelerator Working Group in a different chapter of this report. An understanding of the extent to which such upgrades can contribute to Electroweak Physics has not been fully documented and while reference is made to some possible opportunities the case is not developed in this chapter. Indeed it is one of the recommendations of our report that such studies be pursued.

It may be that some amount of free time will emerge at CERN between the LEP 2 and LHC schedules. If so, this could be used for

- continued LEP 2 running, perhaps at higher energy,
- continued LEP 1 running to gain higher statistics, or
- measurements of A_{LR} using longitudinal polarization at the Z.

Although we allude to some of these possibilities below, the relative strengths of these three possible programs will be determined by the developing physics measurements and machine studies which are carried out over the next few years.

4 Measurements of Electroweak Couplings Near the Z Pole

In this and the following three sections, we will describe the current status of electroweak measurements, their errors, and the prospects for further improvements. A more complete discussion of the physics implications is given in Section 8.

4.1 LEP 1 Results

Over the last four years, the LEP experiments have produced stringent tests of the electroweak theory. Energy scans over the Z peak were carried out in 1990, 1991, and 1993. The 1994 run, like the 1992 run, was devoted to collecting high-statistics data at the Z peak. Under the present schedule, 1995 will be the last year of LEP 1 running before the energy is doubled for LEP 2 running. The specific running plans for 1995 will be determined in late 1994.

The most important tests of the electroweak theory at LEP come from the lineshape parameters (M_Z, Γ_Z, σ_h^0), leptonic and hadronic branching ratios, leptonic forward-backward asymmetries, τ polarization measurements, and branching ratios and asymmetries for $b\bar{b}$ and $c\bar{c}$ events. Within the Standard Model, all LEP measurements can be predicted at tree-level in terms of a single parameter (*e.g.*, $\sin^2\theta_W$ or M_Z). When loop diagrams are included, there are small correction terms depending on M_t (and *very* small corrections depending on M_H). Additional uncertainties arise from the uncertainties in α_s and α_{em} (discussed in Section 2 above) at the Z-pole.

4.1.1 Lineshape

The most precisely measured quantity is M_Z, now measured to a precision of 5×10^{-5}. M_Z is determined from the lineshape, measured from hadronic events taken during energy scans within $\pm$ 3 GeV of the Z peak. The four LEP experiments typically have efficiencies of $> 99\%$ for hadronic events, with an experimental systematic error of $< 0.20\%$. The measurements of both M_Z and Γ_Z are limited by the uncertainty in the LEP beam energy, common to all four experiments. This has been greatly improved during the 1993 scan by exploiting resonant spin depolarization to calibrate the energy at each running point [37]. A precision of about 1 MeV can be attained; this leads to a measurement of E_{cm} to $\pm$ 3 MeV at each running point, limited by the interpolation between calibrations and the greater uncertainty in e^+ energy. The current LEP averages for these quantities are:

$$\begin{aligned} M_Z &= 91.1888 \pm 0.0018 \pm 0.0040 \text{ GeV} \\ \Gamma_Z &= 2.4974 \pm 0.0027 \pm 0.0029 \text{ GeV} \end{aligned} \quad (13)$$

where the errors are statistical and systematic, respectively. The systematic errors are both dominated by the LEP beam energy, which contributes $\pm$ 4 MeV to M_Z and $\pm$ 2.7 MeV to Γ_Z; these errors are now being reduced through work on understanding machine systematics in the 1993 run, and may be further reduced with a possible new scan in 1995.

Normalization of the LEP data, and consequently the measurements of σ^0, Γ_{ee}, and Γ_{inv}, depend on the precision measurement of LEP luminosity; luminosity depends on interaction region as well as time, and is measured separately by each of the experiments. ALEPH, OPAL, and L3 have installed silicon-based luminosity monitors which have reduced the experimental systematic error in luminosity measurement to the level of 0.1%. Each luminosity measurement is currently dominated by the common theoretical uncertainty of 0.25%. This is expected to be improved to the level of 0.10% in the near future, giving a total LEP luminosity error of about 0.15%. The current LEP average of the peak hadronic cross section is [38]:

$$\sigma_h^0 = 41.49 \pm 0.05(\text{exp}) \pm 0.10(\text{theory}) \text{ nb} \quad (14)$$

4.1.2 Leptonic Partial Widths and A_{FB} Asymmetries

The partial widths of the charged leptons at the Z are related to the weak coupling constants by

$$, _{ll} = \frac{G_F M_Z^3}{6\pi\sqrt{2}}(g_{A_\ell}^2 + g_{V_\ell}^2) \qquad (15)$$

Since $g_{A_\ell} \approx -0.5$ and $g_{V_\ell} \approx -0.03$, the magnitude of the partial widths is strongly dominated by g_{A_ℓ}. The forward-backward asymmetries $A_{FB}^{0,l}$ at the Z pole for each lepton flavor l, on the other hand, are sensitive to g_{V_ℓ}, with

$$A_{FB}^{0,l} = \frac{\sigma_F - \sigma_B}{\sigma_F + \sigma_B} = \frac{3}{4}\mathcal{A}_e\mathcal{A}_\ell \qquad (16)$$

and

$$\mathcal{A}_\ell = \frac{2g_{V_\ell}g_{A_\ell}}{(g_{V_\ell})^2 + (g_{A_\ell})^2} \qquad (17)$$

The leptonic partial widths are experimentally determined from $, _Z$ and the leptonic peak cross section by

$$\sigma = \frac{12\pi}{M_Z^2}(\frac{, _{ee}}{, _Z})^2 \qquad (18)$$

and consequently the error on $, _{ll}$ is dominated by the error on $, _Z$. A better quantity to use in global fits to the data is $R_l = , _{had}/, _{ll}$; the errors on R_l are smaller and are uncorrelated with those of other parameters.

Both the relative leptonic partial ratios R_l and the leptonic forward-backward asymmetries A_{FB}^l are dominated by statistics in each experiment and in the combined LEP averages. The systematics in the A_{FB}^l measurements are dominated by charge misidentification and angular resolutions (not correlated between the experiments), and these will improve with better statistics.

The leptonic partial widths of the Z are equal within errors, each measured to a precision of $< 0.5\%$ by combining the LEP experiments. The average of $, _e$, $, _\mu$, and $, _\tau$ gives a mean leptonic partial width $, _l$ measured to a precision of 0.2% with a χ^2/df of 0.2/2.

The measurements of A_{FB}^l are also consistent with lepton universality, but here the agreement is not spectacular, giving a χ^2/df of 5.2/2 . The discrepancy between A_{FB}^μ and A_{FB}^τ is about 2.2 σ; we take this to be consistent with lepton universality.

4.1.3 Tau Polarization

Leptonic couplings can also be measured from τ polarization studies. Because of the V-A coupling in τ decay, the energy and angular distributions of the decay products reflect the polarization of the τ, which is determined by the V and A couplings to the Z of both the initial-state e^+e^- and the final-state $\tau^+\tau^-$. Lepton polarization as a function of production angle is given by

$$\mathcal{P}_\ell = \frac{\sigma_R - \sigma_L}{\sigma_R + \sigma_L} = -\frac{\mathcal{A}_\ell(1+\cos^2\Theta) + 2\mathcal{A}_e\cos\Theta}{(1+\cos^2\Theta) + 2\mathcal{A}_\ell\mathcal{A}_e\cos\Theta} \qquad (19)$$

$\mathcal{P}_\tau$ can be measured in many of the exclusive τ decay channels from the energy distribution of the secondaries (including $e\bar{\nu}_e\nu_\tau$, $\mu\bar{\nu}_\mu\nu_\tau$, $\pi\nu_\tau$, $\rho\nu_\tau$, and $a_1\nu_\tau$). Since the polarization depends on production angle, the data can be used to extract both $\mathcal{A}_e$ and $\mathcal{A}_\tau$. Both measurements are dominated by statistical error, especially $\mathcal{A}_e$; the correlation between the measurements of $\mathcal{A}_e$ and $\mathcal{A}_\tau$ is very small ($\leq 4\%$).

Each of the LEP experiments has combined its own measurements of the various τ decay modes, including correlated systematic errors, to obtain $\mathcal{A}_e$ and $\mathcal{A}_\tau$. In some cases the correlations between modes are small, and in others they are significant. The LEP Electroweak Group has considered systematics common to the experiments (including theoretical uncertainty for the a_1 mode and radiative corrections for hadronic modes), and has found these to be small. V-A coupling for the charged-current decays of the τ has been assumed.

4.1.4 Heavy Flavor Couplings

Since the coupling constants for the heavy quarks c and b are different from those of the leptons (as well as from each other) in the SM, the measurement of the electroweak parameters $A_{FB}^{b\bar{b}}$, $A_{FB}^{c\bar{c}}$, $, _{b\bar{b}}$, and $, _{c\bar{c}}$ provides an important test of the Standard Model. The ability of each of the LEP experiments to separately tag $b\bar{b}$ and $c\bar{c}$ events allows these quantities to be directly measured.

Heavy quarks are tagged using leptons, displaced vertices, and event-shape parameters. Because of the high mass of the b and c quarks, their semileptonic decays give leptons which have a hard momentum spectrum and a large p_t with respect to the parent direction; the larger p_t of the b events allows them to be separated from the c events. Since the long lifetime of hadrons containing b and c quarks gives them decay lengths of a few millimeters, events can also be tagged through the detection of a displaced secondary vertex. New silicon vertex detectors have improved vertex tagging to the point where it is competitive with lepton tagging, especially in measuring $R_b = , _{b\bar{b}}/, _{had}$ and $R_c = , _{c\bar{c}}/, _{had}$. Vertex tagging of b-quarks typically gives an efficiency of 20% with a purity of 90%. Neither lepton nor vertex tagging provides a clean sample of c events. However, a relatively pure sample of c events can be selected by requiring a $D^{*\pm}$ carrying a large fraction of the beam energy.

Double-tagging methods compare the numbers of events with only one hemisphere tagged with the number in which both hemispheres are tagged, and in this way the tagging efficiency is determined from the data. These methods, using tags from leptons, vertices, or both, currently provide the best measurements of R_b.

The LEP Electroweak Working Group has performed a simultaneous fit [38] to R_b, R_c, A_{FB}^b, and A_{FB}^c using data from all experiments. Correlations due to errors

in BR(b$\rightarrow$ l), BR(c$\rightarrow l$), and the mixing parameter $\bar{\chi}$ are fully taken into account. Both R_b and R_c are dominated by systematic errors, while $A_{FB}^{b\bar{b}}$ and $A_{FB}^{c\bar{c}}$ are dominated by statistics. The full heavy flavor electroweak fit gives [39]:

$$\begin{aligned} R_b &= 0.2202 \pm 0.0020 \\ R_c &= 0.1583 \pm 0.0098 \end{aligned} \tag{20}$$

and

$$\begin{aligned} A_{FB}^{0,b} &= 0.0967 \pm 0.0038 \\ A_{FB}^{0,c} &= 0.0760 \pm 0.0091 \end{aligned} \tag{21}$$

The fit gives a correlation coefficient of -0.384 between R_b and R_c; other correlations are negligible. The b parameters have a much higher sensitivity than the c parameters in measuring $\sin^2\theta_W$.

4.1.5 Prospects for Future Improvements

One can anticipate improvements in both statistical and systematic errors in all of the LEP measurements over the next two years. A scan in 1995, with reduced interpolation errors between energy measurements and a better understanding of e^+ energy, should reduce the errors on both M_Z and , $_Z$ to less than 2.5 MeV. The new silicon-based luminosity monitors, combined with improved theoretical understanding of the low-angle Bhabha production, should reduce the error in σ_{had}^0 by a factor of 2.

The total LEP lepton sample, including 1993 data, consists of 700,000 events. One can expect to increase this number by a factor of 2-3 with the 1994 and 1995 runs, with a corresponding improvement in A_{FB}^l. The τ polarization results do not yet include most of the 1993 data, so one can expect a larger improvement in statistics (perhaps a factor of 4). The relative statistical improvement in $b\bar{b}$ and $c\bar{c}$ statistics should be similar. Systematic uncertainties already dominate the R_b measurement, but it is reasonable to expect some reduction in these with more data.

4.2 SLC Measurement of A_{LR}

The quantity $\mathcal{A}_e$ which is determined by the LEP experiments from the forward-backward asymmetry of electron final states and from the angular dependence of the τ final state polarization is directly measured at the SLC with polarized initial state electrons. The left-right asymmetry A_{LR} formed from the total Z production cross sections with left-handed and right-handed electrons, σ_L and σ_R, is simply the product of the beam polarization and $\mathcal{A}_e$,

$$A_{LR} \equiv \frac{\sigma_L - \sigma_R}{\sigma_L + \sigma_R} = P_e \cdot \mathcal{A}_e. \tag{22}$$

The measurement makes use of all Z final states except e^+e^- pairs which have a large cross section from t-channel photon exchange. The principal experimental challenge is to accurately measure the polarization of the electron beam. The SLD Collaboration has used a Compton scattering polarimeter to measure the beam polarization to the 1% level. Since essentially all Z final states constitute the signal, rather simple event selection criteria suppress the backgrounds to a negligible level (0.1%). The measured quantity is independent of acceptance and resolution effects and differs by a small correction (2% for electroweak interference) from the extracted quantity $\mathcal{A}_e$.

The current SLD result [40],

$$\mathcal{A}_e = 0.1637 \pm 0.0071\ (\text{stat}) \pm 0.0028\ (\text{syst}), \tag{23}$$

is dominated by the 1993 measurement which is based upon a sample of 50,000 events logged with 63% beam polarization. The 1994 run is expected to produce a sample of at least 100,000 events with an average beam polarization of 80%. The program is currently expected to run until 1998 and accumulate a total of 500,000 events. The uncertainty on $\mathcal{A}_e$ should decrease by a factor of two at the end of the 1994 run (in Spring 1995) and by an additional factor of two at the end of the program.

5 Measurements of Electroweak Couplings at low Q^2

5.1 Neutrino Measurements of $\sin^2\theta_W$

The first measurements of $\sin^2\theta_W$ came from fixed-target neutrino experiments, which still provide important tests of electroweak theory. Deep-inelastic ν and $\bar{\nu}$ scattering experiments, which measure the ratio R_ν of neutral current (NC) events to charged current (CC) events, have been carried out using narrow-band neutrino beams as well as wide-band beams, both at CERN and at Fermilab. The Q^2 involved in these processes is much smaller than M_Z^2. In the Standard Model, R_ν gives $\sin^2\theta_W = 1 - M_W^2/M_Z^2$; loop-level corrections depending on M_t are quite small [41], and consequently the νN measurement of $\sin^2\theta_W$ is sometimes presented as a measurement of M_W.

5.1.1 Present Status

The most precise measurements have been carried out by CHARM [42], CDHS [43], and CCFR [44]. The dominant systematic error comes from the uncertainty in the effective mass of the charmed quark, which affects the CC cross section through slow-rescaling effects. The CCFR experiment has experimentally measured [45] this effect using opposite-sign dimuon events, obtaining $m_c = 1.31 \pm 0.24$ GeV. When all three experiments are corrected to use this value, the results are quite consistent and give a world average [44] of

$$\sin^2\theta_{\rm W} = 0.2256 \pm 0.0047 \qquad (\nu{\rm N}) \tag{24}$$

or expressed in terms of the W mass,

$$M_W = 80.24 \pm 0.25 \text{ GeV} \qquad (\nu\text{N}) \qquad (25)$$

This is in excellent agreement with the direct measurement of M_W from the collider experiments presented below.

The CHARM II experiment has recently reported the measurement [46] of low-q^2 leptonic neutral current couplings from $\nu_\mu e$ scattering. They obtain

$$\sin^2\theta_W = 0.2324 \pm 0.0058 \pm 0.0059 \qquad (\nu_\mu e) \qquad (26)$$

where the first error is statistical and the second systematic. This is a purely leptonic process; the results agree well with high-q^2 leptonic processes ($e^+e^- \rightarrow l^+l^-$) at LEP.

5.1.2 Future Prospects

E815 (using a modified CCFR detector with a new collaboration) is scheduled to take high-statistics νN data in the next Fermilab fixed target run. By running alternately with ν and $\bar{\nu}$ beams, the collaboration hopes to improve the measurement of $\sin^2\theta_W$ to a precision of ± 0.0032 (equivalent to a resolution of ± 165 MeV on M_W), and also to measure ρ to a precision of 0.5%.

5.2 Atomic Parity Violation Measurements

Atomic parity violation experiments were among the first searches for the weak neutral current. Since it does not conserve parity, the weak neutral current can mix atomic states of (nominally) opposite parity. This implies that electric dipole (E1) transitions can occur between atomic states which are nominally same-parity eigenstates. The amplitudes for such forbidden transitions $\mathcal{E}_{PNC}$ can be expressed as

$$\mathcal{E}_{PNC} = C_{PNC} \cdot Q_W({}^A_Z N), \qquad (27)$$

where the factor C_{PNC} contains the detailed atomic physics and the factor Q_W is the weak-charge of the atomic nucleus ${}^A_Z N$,

$$Q_W({}^A_Z N) \equiv \rho\left\{Z - N - 4Z\sin^2\theta_W\right\}, \qquad (28)$$

where Z and N are the proton and neutron numbers of the nucleus, respectively, and $A \equiv N + Z$ is the mass number.

The electroweak radiative corrections to the weak charges of heavy nuclei have the interesting property [47] that the corrections to the ρ parameter nearly cancel. The remaining corrections depend mostly upon the S parameter which makes this class of measurements somewhat unique. Unfortunately, direct determinations of Q_W are limited by the precision of the calculations for the C_{PNC} factors.

A number of researchers have discussed eliminating the sensitivity to these factors by measuring the PNC amplitudes for several isotopes of the same atom [48]. Measurement of the ratio $\mathcal{E}_{PNC}({}^A_Z N)/(\mathcal{E}_{PNC}({}^{A'}_Z N) - \mathcal{E}_{PNC}({}^A_Z N))$ cancels the factor $C_{PNC}\rho$ which eliminates the atomic physics uncertainty but also destroys the approximate T cancellation. The SM information (S-T trajectory) determined by the ratio is identical to that provided by the measurement of $\sin^2\theta_W^{eff}$ at the Z pole.

5.2.1 Present Status

At the current time, the most precise Standard Model information is extracted from the 2% measurement of the 7S-6S transition in ${}^{133}_{55}$Cs [49,50,51],

$$\begin{aligned} Q_W({}^{133}_{55}\text{Cs}) &= -71.04 \pm 1.58 \pm 0.88 \\ S &= -3.0 \pm 2.1 \pm 1.2, \end{aligned} \qquad (29)$$

where the first error is experimental and the second is theoretical; the latter is due to the 1% uncertainty in atomic physics calculations for Cs [50]. The measured value of S is consistent, within the rather large errors, with the Standard Model expectation of $S \approx 0$.

Very recently, parity-non-conserving amplitudes for E1 transitions in Bi, Pb, and Th have been measured [52] with 1% precision. Unfortunately, these atomic systems are more complex than cesium and comparably precise calculations of the C_{PNC} factors do not exist, but are being pursued for the thallium system [53].

5.2.2 Future Prospects

In the near term future, the Cs measurement at Colorado is expected to improve by at least a factor of four [54]. The work on lead and thallium at Washington and Oxford is continuing with measurements on pure isotopes. New measurements on francium [55] and dysprosium [56] are being undertaken at Stony Brook and Berkeley, respectively. An improved calculation of the C_{PNC} factor for the Cs transition is difficult but may yield a result with a 0.2-0.4% precision [53]. The situation for the francium system is similar except that it will be necessary for the experimentalists to measure a number of atomic properties as cross checks. The field is therefore at something of a crossroads. In the next few years, it is expected that S can be measured to the level of $\pm$ 0.5 .

In the longer term, progress is likely to come from measurements of multiple isotopes (although as discussed above these measurements introduce a T dependence). The ultimate precision of such measurements is not clear at the current time.

6 Measurements of the W-boson Mass

A critical test of the Standard Model is the comparison of M_W predicted by the quark and lepton couplings with the direct measurement of M_W. As discussed in Section 8, this provides a direct test of electroweak quantum corrections, potentially more exacting than that provided by the top quark. In order to provide the most stringent test, the resolution in the direct measurement of M_W should match the precision of LEP measurements; this requires a resolution of ~40 MeV,

6.1 Present Status: Tevatron Measurements

Precise measurements of M_W have been made by UA2, CDF, and DØ . Event selection for both CDF and DØ consists of requiring a high-p_t lepton ($p_t > 25$ GeV/c) and large missing transverse energy ($E_t > 25$ GeV). Event selection is quite clean, with backgrounds at the level of a few percent. The measurements from both CDF and DØ are based on a maximum likelihood fit of the transverse mass distribution of W candidates. The errors in the mass measurements quoted by both experiments consist of three components: statistics, systematics, and scale.

The CDF scale error is based on a measurement of the J/ψ mass with J/$\psi \to \mu^+\mu^-$ decays using the magnetic field. That mass is then scaled to the particle data group value for the mass of the J/ψ. A check on the higher momenta is provided by the Υs and Zs but is not used to scale the value. For muons, this results in a scale error of 60 MeV. For electrons, calorimetric energy is used, with the energy scale determined from the tracking scale and the measured E/p distributions. The scale error for electrons is then 130 MeV. The dominant non-scale systematics include ±120 MeV from momentum resolution, ±90 MeV from the uncertainty in the p_t of the underlying event (based on Z production studies), and ±100 MeV from uncertainties in structure functions. At the present time, these errors are preliminary and are expected to be reduced before final publication [57]. The CDF results are:

$$\begin{aligned} M_W^e &= 80.47 \pm 0.15 \pm 0.21 \pm 0.13\,\text{GeV} \\ M_W^\mu &= 80.29 \pm 0.20 \pm 0.22 \pm 0.06\,\text{GeV} \end{aligned} \quad (30)$$

where the three errors are due respectively to statistics, non-scale systematics, and scale uncertainties. These measurements are combined, taking into account common errors, to give:

$$M_W^{e+\mu} = 80.38 \pm 0.23 \text{ GeV} \quad (\text{CDF, 1994}) \quad (31)$$

DØ has presented [58] an M_W measurement based on $W \to e\nu$ events only; with no central magnetic field, their electron data provide the best measurement of M_W. The DØ scale error is based entirely on Z events within the same fiducial region of the calorimeter. A fit allowing for a slope and constant term in the electron energy response gives an error of ±260 MeV. Inclusion of lower mass resonances, the J/ψ and π^0, reduces this to 185 MeV. This reduction and others will be reflected in the final published result for 1994. Other systematics, comparable in size to those of CDF, give a non-scale systematic error of ±160 MeV.

$$\begin{aligned} M_W^e &= 79.86 \pm 0.16 \pm 0.16 \pm 0.26\,\text{GeV} \\ &= 79.86 \pm 0.35 \text{ GeV} \quad (\text{DØ, 1994}) \end{aligned} \quad (32)$$

The errors in the first line are due respectively to statistics, non-scale systematics, and scale uncertainties.

The world average of these measurements, combined with the earlier UA2 [59] and CDF [60] measurements is [61]

$$M_W = (80.23 \pm 0.18)\,\text{GeV} \quad (\text{World Av., 1994}) \quad (33)$$

where the combination assumes common errors of ±100 MeV.

6.2 Future Prospects

6.2.1 The Tevatron

Each of the three Tevatron measurements of M_W from Run 1a has a statistical error in the range 150-200 MeV. Scaling to 100 pb^{-1} and 1000 pb^{-1} gives statistical errors of ~90 MeV and ~30 MeV for Run 1b and Run 2 respectively for each measurement. In addition, DØ will expand their η coverage to gain a factor of 1.5 in W statistics.

The scale errors in both tracking and calorimetry rely on calibration to a well known resonance, and in all cases the errors should improve approximately as $1/\sqrt{N}$ with higher statistics. For example, higher J/ψ statistics improves the checking of the spatial variations in the field integral for CDF, and higher Z statistics improves the calibration of the DØ calorimetry.

The systematic errors comprise a list of more than ten effects each of which is already smaller than 100 MeV. About three quarters of these effects are limited by the statistics in the data for W's and Z's and are instrumental in origin. The remaining errors are quasi-theoretical in nature and are associated with the details of the production process. In the case of the W p_t spectrum, the Z spectrum is expected to provide the appropriate check. The structure function effects are controlled in part through the measurement of the W asymmetry. The use of this constraint [62] will be implemented in future analyses, and may give a significant reduction in the systematic error from structure functions. It is an important step away from reliance on measurements which

need to be carried over from other processes and evolved to the appropriate scale.

The most important point to realize is that no "brick walls" have yet been identified above 30 MeV. We therefore assume that systematic errors will continue to decrease with increasing statistics, but not as fast as do statistical errors. After 100 pb^{-1}, three measurements of M_W with an expected precision of about 150 MeV each and common errors of 70 MeV lead us to expect an overall error of about 110 MeV. For a 1 fb^{-1} exposure with the Main Injector, one would estimate an error of approximately 60 MeV per measurement, of which 35 MeV are common. With four measurements, two from each experiment, a resultant precision of approximately 50 MeV is possible.

Reasonable expectations for the error on M_W, from CDF and DØ combined, are 110 ± 20 Mev after 100 pb^{-1} and 50 ± 20 MeV after 1000 pb^{-1} from the Tevatron measurements.

6.2.2 LEP 2

The center of mass energy of LEP 200 is expected to be at least 10 GeV higher than W pair threshold. The studies referred to in this section assumed 190 GeV and an integrated luminosity of approximately 500 pb^{-1} from about 3 years or so of running.

In principle the mass of the W boson can be measured at LEP 200 by either reconstruction of the final state of hadronic and leptonic decays of the W bosons, or through measurement of the excitation curve for the process. The procedure common to both measurements is that of event selection. W pair production is by no means the dominant process and a careful selection must be made to reduce the backgrounds from conventional annihilation into hadrons and other processes. Care must be taken to handle the radiative effects which rob the initial state of energy but for which the radiated photon appears in the detector. Although the different techniques give comparable precision, it is unlikely that the excitation curve approach will be used since it requires substantial running very low on the threshold curve and hence with diminished event yield.

Reconstruction of events in which one of the W's decays leptonically, as well as those in which both decay hadronically, may be used in the analysis. At some level the leptonic reconstruction and the hadronic reconstruction give independent measurements. According to Monte Carlo studies [63], in either case, reconstruction of the masses results in values lower than that generated. This is attributed to energy lost during reconstruction. The typical shifts are a few GeV and the distributions are of order 10 GeV wide. In order to correct for this, use is made of the beam energy constraint; the resultant masses are rescaled by the ratio of $E_{beam}/E_{W,Recons}$. The resultant distributions are much narrower and are about 200-300 MeV lower than the input mass.

The final correction, of the order of a few hundred MeV, must be made using careful Monte Carlo studies. One component is due to radiative corrections and is well understood. That due to mis-reconstruction will have an error estimated to be about 30 MeV. In addition there is a final error of about 20 MeV, common to all methods and to all experiments, from knowledge of the beam energy. This is the major contributor to an expected overall common error of about 30 MeV. Thus there are potentially 8 measurements each with about 50 MeV overall error. With the common error taken into account, a best estimate for an overall LEP 2 precision based on these Monte Carlo studies would be $\delta M_W = 40$ MeV.

6.2.3 Other Possibilities (TeV*, LHC, NLC)

As we describe in Section 8.6 below, an improvement in δM_W from 40 MeV to 20 MeV would provide a better match to the expected resolutions on M_t and other electroweak measurements expected over the next decade. This would also significantly improve the resolution of the predictions of the Standard Model Higgs mass from global electroweak fits. It is not clear that an M_W resolution as low as 20 MeV can be achieved, but with a dedicated effort one can probably do better than the 40 MeV we have estimated. At LEP 2 this might be possible through improvements in beam energy measurement (using resonant depolarization closer to the beam energy [64]) and increased integrated luminosity in an extended LEP 2 program. Both LHC and the Tevatron may also be able to surpass 40 MeV, but it will be exceedingly difficult to achieve the necessary improvements in systematic errors.

The determination of M_W has been discussed [65] for an e^+e^- linear collider. The beam energy precision is not as good as at LEP 2 so that particular constraint is not available; the statistics are however rather high. At 500 GeV with 100 fb^{-1}, approximately 80K events of the type $e^+e^- \to e\nu W$ would be reconstructed. The statistical error is then less than 20 MeV. Calibration would use about 40k $e^+e^- \to \gamma Z$ events in the same fiducial region in conjunction with a calibration run at the Z pole.

6.3 Other Aspects of W Physics

The couplings of the W to other particles are additional parameters which are predicted by the Standard Model and which can be determined from the measured partial widths of the W to specific final states. Deviations from the SM predictions could signal new decay modes (*e.g.*, $W \to t\bar{b}$ for a light top) or loop corrections involving new particles or new couplings. Both , $_W$ and $B(W \to l\nu) =$

, $(W \to l\nu)/$, $_W$ have been measured in hadron collider experiments.

Indirect measurements [66,67,68] of $B(W \to l\nu)$ have been carried out by UA1, UA2, CDF, and DØ using the measured event ratio $R = \sigma B(W \to l\nu)/\sigma B(Z \to l^+l^-)$, multiplied by the theoretical production cross-section ratio $\sigma(p\bar{p} \to Z)/\sigma(p\bar{p} \to W)$ and the LEP measurement of the branching ratio $B(Z \to l^+l^-)$. The published world average [11] for the leptonic branching ratio is $B(W \to l\nu) = 0.107 \pm 0.005$, to be compared with the Standard Model expectation [69] of 0.1084 ± 0.0002. The agreement between the measurement and theory has been used by both CDF and DØ to exclude a light top ($M_t < 62$ GeV) in a way which is independent of any assumptions about top decay modes. In the future, the error in $B(W \to l\nu)$ is likely to be limited at about the 1% level by the theoretical uncertainty in the production cross-section ratios (note that the quantity actually measured here is $B(W \to l\nu) \times \sigma(W)/\sigma(Z)$).

CDF has recently presented [70] a direct measurement of the W width , $_W$ based on the measured shape, and especially the high-mass tail, of the transverse mass distribution of $W \to e\nu$ events. In the region far above M_W the effects of the largely gaussian resolution of the detector die off and the distribution is determined by the Breit-Wigner distribution of M_W. From the data of Run 1a, CDF obtains , $_W = 2.11 \pm 0.28(stat) \pm 0.16(syst)$ GeV. The systematic error comes from measured detector resolutions, and consequently both errors should improve with statistics approximately as $\sqrt{N}$. After 1 fb^{-1} of data (Run 2), an error in , $_W$ of about 30 MeV is expected [70] from CDF and DØ combined; this precision approaches the level of radiative corrections to the width.

Furthermore, the direct measurement of the W width may be combined with the leptonic branching ratio measurement to provide a measurement of , $(W \to l\nu)$. This leptonic partial width is predicted to be , $(W \to l\nu) = g^2 M_W/48\pi$, and thus its measurement may be used to determine g. In conjunction with the measured leptonic branching ratio, this would give a measurement of , $(W \to l\nu)$ at the 1.8% level, and consequently an error on the W-$l\nu$ coupling g of 0.9%. The extraction of g from , $(W \to l\nu)$ is more reliable because it is not sensitive to QCD corrections that are present in the , $(W \to q\bar{q})$ widths.

7 The Top Quark

The most exciting recent result in high-energy physics has been the first evidence [2] for the top quark, presented in April 1994 by the CDF Collaboration and based on the data from Run 1a. A measured cross section of $\sigma_{t\bar{t}} = 13.9^{+6.1}_{-4.8}$ pb from dilepton and lepton+jet events was reported, with an estimated mass for the top quark

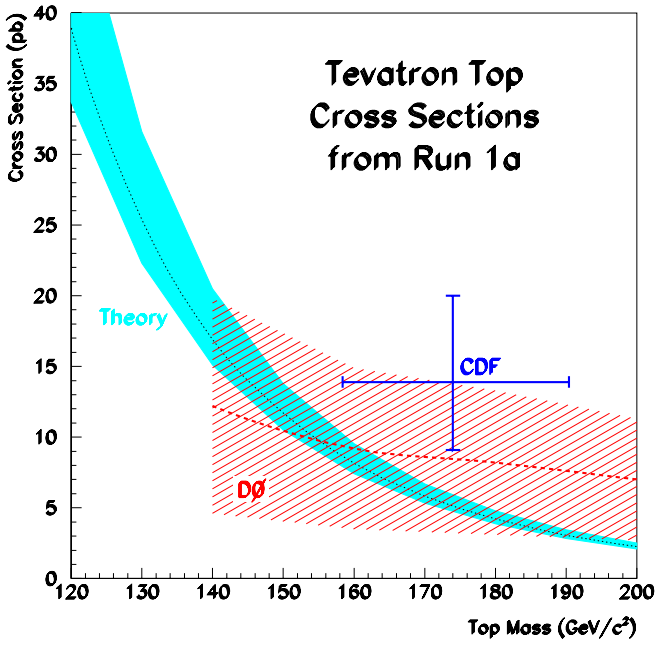

Figure 1: Top cross section versus M_t. The solid band is the theoretical NNLO prediction, the cross-hatched region is the 1-σ range from DØ and the point is the measurement from CDF. The horizontal error bar on the CDF point comes from the mass estimation from lepton+jet events. DØ does not report a measurement of the mass.

of $174 \pm 10(stat) \pm 12(syst)$ GeV based on the reconstruction of lepton+jet events. The DØ experiment reports no significant signal [71,72]. In terms of cross section, the DØ result is $\sigma_{t\bar{t}} = 8.2 \pm 5.1$ pb if a mass of 180 GeV is assumed. The two reported cross sections are compatible both with each other and with the expectations of the Standard Model [73], as shown in Figure 1.

Although the statistical significance of the data, from Run 1a only ($\sim$ 20 pb^{-1}), is too limited at present to unambiguously establish the existence of the top quark, the Fermilab data sample has already doubled in Run 1b. It will double again within the next year, and with a continued high level of accelerator performance it is expected to reach a total of 160–200 pb^{-1} for Runs 1a and 1b combined. If $\sigma_{t\bar{t}} \geq 5$ pb (less than the central value reported by either experiment, and corresponding to the theoretical prediction for $M_t \approx 180$ GeV), then each experiment would expect to see a signal of at least 2-3 σ with 100 pb^{-1} of luminosity. A Standard Model top with a mass even as high as 200 GeV, which is at the edge of consistency with present data from Fermilab and LEP, should be definitively measured with 200 pb^{-1}.

It is clear that the accumulation of high statistics at the Tevatron deserves the highest priority. The importance of the discovery of the top quark is three-fold. First, the top is an essential element of the basic SU(2)

structure of the Standard Model. Its discovery is crucial for us to claim to have fully established the basic elements of the theory; if the top were not found the Standard Model would have to be rejected or drastically modified.

Secondly, the top quark has effects on other measurable parameters of the Standard Model through higher-order loop diagrams. These effects are calculable as a function of M_t, and their measurement provides a major test of the renormalization structure of the Standard Model and of the quantum effects predicted by the theory. The essential ingredient for these tests is a precise measurement of the mass of the top quark, discussed below.

Finally, the only property of the top quark for which we now have direct evidence is its mass, and this might be regarded as anomalously high (more than an order of magnitude above the mass of any other quark or lepton); it may well be that other properties of the top quark hold additional surprises. Moreover, the top mass is on the scale of electroweak symmetry-breaking; this makes the top a potential laboratory for studying symmetry-breaking effects and for finding possible new particles or new effects in top decays that might take us beyond the Standard Model. The essential ingredient for these investigations is a thorough study of all accessible parameters of the top quark, including its V and A coupling strengths, and its width, decay modes, branching ratios, and production mechanisms.

7.1 Current Status of the Direct Measurement of M_t

The cross section $\sigma_{t\bar{t}}$ is an imprecise indicator of M_t, and using it would in any case introduce a theoretical bias which should be avoided. Consequently the determination of the top mass must be based on the reconstruction of $t\bar{t}$ events, and is sensitive to event reconstruction, detector resolution, particle identification, and backgrounds.

Each $t\bar{t}$ final state is expected to decay into $b\bar{b}W^+W^-$, with each W decaying into either $l\nu$ ($BR = \frac{1}{3}$) or qq' ($BR = \frac{2}{3}$). Events with two leptonic W decays are quite distinctive, but at the present level of statistics they do not allow an accurate reconstruction of M_t due to the missing neutrinos. Events with two hadronic decays might allow mass reconstruction, but at present they cannot be separated from the large backgrounds. Events with one leptonic decay and one hadronic decay have a distinctive signature from the high-p_t lepton and sufficient information from the hadronic decay to allow a reconstruction of the parent top mass. The CDF measurement of the top mass is based solely on events of this lepton+4-jet topology.

The CDF analysis starts with a sample of 52 W + 3-jet events, and selects the subsample of 10 events which show a b-quark tagged by either a displaced vertex or a final-state lepton. The jet identification criteria are then relaxed for the 4th jet to obtain higher acceptance, giving a subsample of 7 events with 4 jets and a b-tag. The background in this sample, obtained by using Monte Carlo calculations to extrapolate from 3-jet data, is estimated to be $1.4^{+2.0}_{-1.1}$ events. Each jet is then identified with one of the final-state quarks, and a constrained fit is carried out allowing the measured energies and angles to vary within experimental errors and under the constraints that the b-tagged jet be assigned to one of the b quarks, that the two jets assigned to the W reconstruct to M_W, and that the reconstructed masses of the t and $\bar{t}$ be equal. The assignment of jets giving the best χ^2 is used to calculate the value of M_t for that event. The distribution of reconstructed masses is compared to Monte-Carlo expectations in Figure 2.

The number of possible jet permutations for each event is large and the situation is exacerbated by the presence of initial and final state gluon radiation; the requirement of the b-tag reduces the number of viable combinations by a factor of 2. Nevertheless, from Monte-Carlo studies the CDF group finds that the assignment of jets giving the best χ^2 gives a wrong solution about two-thirds of the time. This produces a smearing of the mass resolution relative to that for correct solutions, while apparently leaving the central value unshifted. This is demonstrated for Monte Carlo events in Figure 3. The width of the Monte Carlo distribution suggests that the effective σ is in the range 20-25 GeV for a single event; this agrees with the quoted statistical error of ± 10 GeV on M_t. The central value and the errors on M_t are obtained from maximum likelihood fits to the data, using admixtures of the postulated top signal and estimated backgrounds, as shown in the inset in Figure 2.

The major systematic errors [2,74] are due to uncertainties in (a) the energy scale of the detector (1.8%), (b) the effects of gluon radiation on measured jet energy (4.4%), and (c) the shape assumed for the background ($^{+5.3}_{-4.4}$%).

Both (a) and (b) affect the assignment of momenta to the final state jets, so systematic errors here have a direct effect on the reconstructed top mass. The question of gluon radiation from jets is particularly important because parton quantities are required to calculate the mass of the top. A check of the systematics, and a possible correction for any bias, is provided by the hadronic W decay in the top event sample and also by other data samples such as γ + 1-jet events. In general, systematic uncertainties in the reconstructed jet energy are obtained from the data and should scale as $1/\sqrt{N}$ for the foreseeable future.

The other significant source of systematic error (c) is due to errors in the assumed shape of the background from QCD events and from W+jets production. When

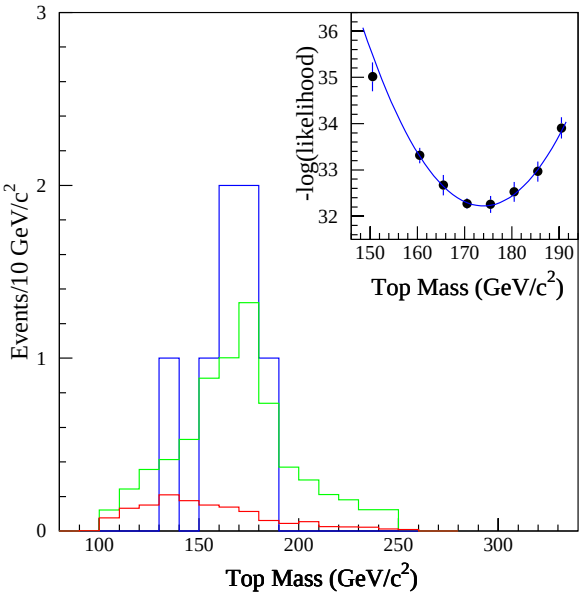

Figure 2: Top mass distribution for CDF data. The solid histogram is the data, the dotted histogram indicates the estimated W+jets background. The dashed histogram is the sum of the appropriate numbers of Monte Carlo signal and W+jets background.

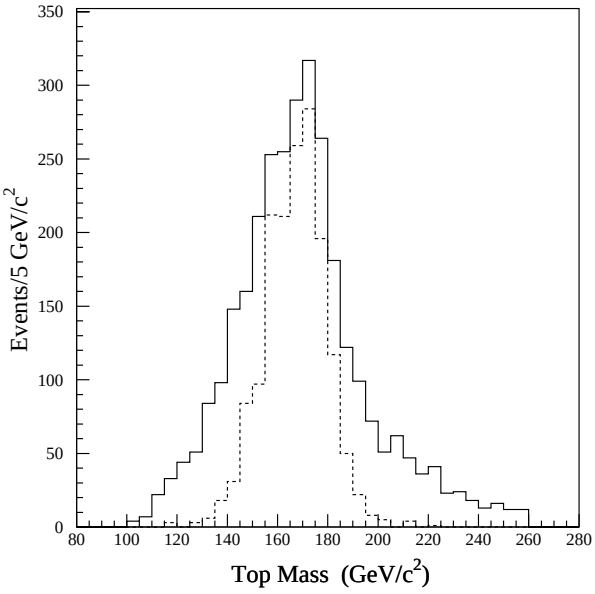

Figure 3: Monte Carlo showing the best χ^2 solutions as a function of mass when one of the b jets is correctly identified. The dotted line indicates the distribution of correct solutions.

fitted to the top hypothesis, the background tends to peak at masses near 140 GeV, as shown in Figure 2. The higher the top mass, the less this is important and, as sample sizes increase, more sophisticated discriminators can be used. Studies of $W+n$-jet events will clearly help in understanding backgrounds and reducing systematic errors; these studies will improve with higher statistics.

7.2 Future Measurements of M_t

7.2.1 M_t at the Tevatron

As discussed above, the systematic errors in M_t are expected to decrease with increasing statistics, roughly as $1/\sqrt{N}$ in the near future. Consequently, one might naively extrapolate the future error on M_t by scaling from the present CDF error of ± 16 GeV. This would give an expected top resolution of $\sim$8 GeV after 100 pb^{-1} and, allowing for a slower reduction in systematic error during Run 2, perhaps $\sim$4 GeV after 1000 pb^{-1}. This extrapolation procedure predicts a satisfying factor of two reduction after each subsequent run, and it has the overwhelming advantage of simplicity; but it neglects a number of important factors.

At present, the only measurement of M_t comes from the CDF data of Run 1a. As discussed above, we expect a clear top signal to emerge in both detectors in Run 1b if $M_t < 200$ GeV, and the total Tevatron data sample will consequently be enhanced over that of CDF alone. Improvements in acceptance and the inclusion of additional channels and new analysis techniques will lead to additional improvements. On the other hand, there are still large statistical limitations in our understanding of both $\sigma_{t\bar{t}}$ and M_t, so projections of future precision are necessarily uncertain.

Consequently we consider the scenario of $\sigma_{t\bar{t}}$=5 pb, which would correspond to the theoretical cross section for M_t=180 GeV. We assume slightly improved efficiencies for b-tagging and for acceptance and include a 30% loss in efficiency from the 4-jet requirement. We use an efficiency$\times$branching-ratio of $\sim$5% summed over CDF and DØ. If M_t is determined only from events with 4 jets plus a b-tag, then with 100 pb^{-1} of data we find approximately 25 events from both detectors combined. Assuming a resolution of 25 GeV from each event gives a statistical error of 5 GeV on M_t. With the additional assumption that systematic errors in jet energy and in background subtraction will scale as $1/\sqrt{N}$ during Run 1b, we obtain a systematic error of $\sim$6 GeV, giving a final error on M_t of $\sim$8 GeV[c]These estimates have

[c]Note added in proof: In March 1995, CDF and DØ each presented definitive confirmation ($> 4\sigma$) of the existence of a massive top quark. The CDF mass was $176 \pm 8 \pm 10$ GeV, and the DØ result was $199^{+19}_{-21} \pm 22$ GeV. Both systematic errors are expected to improve with additional analysis work. These results are completely in accord with the expectations discussed in this report.

been based on events with lepton+jets(with b tag). Additional information will come from non-tagged events, selected through kinematic analyses with backgrounds suppressed with event shape cuts, which appear to have only a slightly broader mass distribution than the tagged events [75]. The di-leptons have also been shown to have potential for mass determination [72,76] which we have not included. We conclude that a mass resolution of 8 GeV on M_t is a reasonable projection for the end of Run 1b. It may well be that this estimate will be surpassed with new analysis techniques or a larger event sample.

It is likely that systematic errors will improve more slowly than statistical ones as the data sample increases beyond 100 pb^{-1}. But before the beginning of Run 2, there will be significant upgrades to both detectors in addition to the critical upgrade in luminosity provided by the Tevatron Main Injector. DØ will install a solenoid and a silicon vertex detector before running with the Tevatron Main Injector, and CDF has a program for upgrading its muon and calorimeter systems as well as for installing an upgraded silicon vertex detector. Both systematic and statistical errors should be improved by these upgrades. We believe a resolution of 4 GeV on M_t by the end of Run 2 is a reasonable extrapolation from present knowledge.

As is the case with W mass measurements, there are no "brick walls" to absolutely limit improvement in the resolution of M_t. Additional running should lead to improvements in systematic as well as statistical error (although perhaps not as fast an $1/\sqrt{N}$), and so an extended high-luminosity run of 10 fb^{-1}, using an upgraded Tevatron such as TeV*, will further improve δM_t. But the uncertainties in our projections are already large, and there seems little point in trying to estimate the size of further improvements until we know more about the properties of the top and have more experience with the application of different analysis techniques to a larger data sample. This is another important reason for trying to maximize statistics in Run 1b.

7.2.2 M_t at the LHC

Top production at the LHC proceeds through gluon fusion 90% of the time and is complementary to the Tevatron where quark antiquark annihilation dominates. The $t\bar{t}$ production cross section at LHC will be about 300 times greater than that at the Fermilab Tevatron; at equal luminosities of 10^{32} cm^{-2}sec^{-1} (1.0 fb^{-1}/year), one day of LHC will produce as many $t\bar{t}$ events as one year of Tevatron running. With LHC running at 10 fb^{-1}/year (one tenth design luminosity), one year should produce $> 10^7$ $t\bar{t}$ events (for $M_t \leq 200$ GeV). This will make it possible to study decay modes with very small branching ratios. We describe two methods for measuring the top mass that have been examined by the ATLAS [77] and CMS [78] collaborations.

The first method uses lepton+jet events, requiring an isolated lepton with p_t >40 GeV from $t \to bW, W \to l\nu$, with three jets in the opposite hemisphere from $\bar{t} \to b\bar{W}$, $\bar{W} \to$ 2 jets. The top mass is reconstructed from the three jets, requiring that two of them reconstruct to a W and that the third be tagged as a b-jet using its displaced vertex. Backgrounds from W+jets are large, but can be greatly reduced by requiring a tag for the second b-jet. Poor statistics are not at issue: 1.0 fb^{-1} should give a statistical error of less than 1 GeV, so the statistical error is small and one can apply additional cuts to obtain a cleaner sample of events. The LOI's [77,78] for ATLAS and CMS estimated a precision of $\leq$ 5 GeV. More recent work [79] indicates that an error of $<$ 3 GeV can be attained for $M_t = 175$ GeV. As in the case of the Tevatron, the jet reconstruction scale is expected to be established by the hadronic W decays in the top event sample.

The second method requires both W's to decay leptonically, and for one of the $b's$ to decay semileptonically. The mass distribution of the $l\bar{l}$ in the same hemisphere (from the same parent t) can be used to determine the t mass. This method should work even at high luminosities, when jet energy measurement is worsened by the high event rate. This method requires integrated luminosities of 10 fb^{-1} or more, but provides an important alternative procedure which is independent of the energy scale of jets. The method is calibrated by Monte Carlo simulation of the leptonic decays. Recent studies [80] indicate that a resolution of $\leq$ 2.5 GeV can be attained for $M_t = 175$ GeV.

Since there will be two experiments with comparable resolutions, a precision on M_t of 2 GeV seems achievable after about two years of LHC running.

7.2.3 M_t at the NLC

The most precise measurements of the top mass which have been considered are those done at a proposed linear e^+e^- collider (NLC), with a center of mass energy which can be varied from below $t\bar{t}$ threshold to 500 GeV and with an integrated luminosity of ~50 fb^{-1} per year. Two methods for measuring M_t have been discussed [81].

A nine-point scan over the threshold region, using a total integrated luminosity of 10 fb^{-1}, is expected to yield resolutions of 300 MeV for M_t=150 GeV and 520 MeV for M_t=180 GeV [81]. The determination of M_t uses both the measured excitation curve and the momentum distributions of the top at each scan point. Cuts selecting lepton+4-jet events were used for the momentum measurements, giving about 15% efficiency and negligible backgrounds.

At energies of 100 GeV above $t\bar{t}$ threshold, M_t can be reconstructed from both 6-jet and 4-jet+lepton final states. Selection cuts yield efficiencies of ~30% with

background levels of ~10%. A statistical precision of ~150 MeV can be obtained with 10 fb^{-1}. There are systematic shifts of ~500 Mev from various sources which must be taken out, and residual systematic uncertainties of also ~500 MeV; it is thought that both of these can be reduced in the future. Although the threshold scan probably yields the better precision, the high-energy data give very different systematics and provides an important check of M_t (as well as additional information as described below).

7.3 Other Aspects of Top Physics

The mass of the top quark is anomalously high, being on the order of the electroweak symmetry-breaking scale rather than on the mass scale of other quarks. This makes it especially important to measure other properties of the top with the best precision possible. These properties include the decay modes, branching ratios, width, couplings, and production cross sections.

A detailed study of the top quark is envisaged as a major part of the program for an e^+e^- linear collider [81,82]. However, a subset of such studies may also be accessible to higher luminosity running at the Tevatron and at LHC. Studies of these programs are underway for both LHC [77,78] and the Tevatron [83,84].

7.3.1 Top Physics at Hadron Colliders: LHC and TeV*

At both the Tevatron and the LHC, a number of important quantities can be determined from the final states of $t\bar{t}$ events, with precision mainly limited by statistics. The measurements needed include partial widths which may rely heavily on double B-tagging capability and multiple lepton detection and momentum determination. Techniques [85,86] exist for determining the ratio of $V-A$ to $V+A$ decay couplings using for example the correlations between the b and the lepton (from the same t) in lepton+3-jet events. These require accurate determination of the b quark direction and a reliable algorithm for reconstruction of the W four-momentum. Such studies are especially interesting for the top since it decays primarily into $b-W_{long}$, rather than through the W_L polarization state which dominates all weak decays of lighter particles. From the statistics expected in Tevatron Run 2, it is expected that the branching ratio to W_{long} can be measured to a precision of better than 10% [86]. A CP violation test is also possible in top pair production by determining the spin component perpendicular to the plane formed by the b and lepton [85,87].

The single-top "W-gluon-fusion" production mechanism ($W^+g \rightarrow t\bar{b}X$) is a source of complementary top physics [88,89]. This process occurs through a strictly electroweak mechanism, and since the t is produced in association with a light $\bar{b}$, each particle is produced in a pure negative-helicity state; measurement of the energy and angular distributions of the b resulting from t-decay therefore determines the relative $V-A$ and $V+A$ charged-current couplings of the top (expected to be pure $V-A$). Moreover, since this process occurs through the $W-t\bar{b}$ vertex it provides a measurement of the magnitude of this coupling and consequently gives the total width of the top quark. The cross section for $t\bar{b}+\bar{t}b$ is roughly half that of $t\bar{t}$; detection efficiencies using conventional cuts are estimated to be ~20% those of $t\bar{t}$. Initial studies [89,90] have indicated that backgrounds from W+2-jet events in this channel are severe, which may limit its importance. Additional studies are under way [84].

At equal luminosities of 10 fb^{-1}, the number of reconstructed $t\bar{t}$ events produced should be about 5,000 for TeV* and on the order of 500,000 for the LHC. Although the LHC has a clear statistical advantage, one should note that the relative mix of $q\bar{q}$ and gg production mechanisms is quite different for $p\bar{p}$ (Tevatron) versus pp (LHC) colliders. At the LHC, gg production of $t\bar{t}$ will dominate while at the Tevatron, $q\bar{q}$ production will dominate. The two machines are consequently different both in backgrounds and in the physics of top production.

7.3.2 Top Physics at a Linear e^+e^- Collider (NLC)

The NLC would provide a number of advantages in top studies: a clean environment, control of E_{cm} (in the $t\bar{t}$ frame), and the ability to run with polarized beams. Although statistics are small compared to those of the LHC, systematics and backgrounds are much better. As described above, a threshold scan can determine M_t to $\pm$500 MeV; the same scan could provide a measurement of the width of the t to a precision of 5-10% [91].

In a run at energies ~100 GeV above $t\bar{t}$ threshold, the t and $\bar{t}$ quarks produced will be highly polarized due to the interference between the electromagnetic and weak currents, and the fast decay of the top via the weak charged current will preserve the helicity information [81,82]. Semileptonic decays can be reconstructed to determine the helicity structure of *both* the production (neutral current) and decay (charged current) couplings simultaneously. Control of the polarization of the beams would increase the sensitivity of these measurements.

A run of 50 fb^{-1} at E_{cm}=400 GeV is expected to produce about $10-15\times10^3$ reconstructed events, and to allow the measurement of each of the SM couplings to the level of a few percent. The anomalous magnetic moment could be measured to ~0.02 Bohr magnetons, compared to the expected moment of α_s/π=0.04 from QCD [81].

7.3.3 Beyond the Standard Model

Since the top is the heaviest of the known elementary particles, its decays may produce states which have not been observed previously. At any of these potential top factories, a number of non-standard model searches are possible with a sufficient top sample. Within supersymmetric models, additional light Higgs-like particles are required which would naturally couple to the heaviest particles: decay from the top, $t \to bH^+$ and subsequent decay to tau leptons. This could conceivably occur at a rate of 10% of the conventional one. SUSY also requires the existence of a scalar top SUSY partner which could be produced at sizable fractions of the rate of conventional top and would have a similar signature. These and other effects are discussed in the "Beyond the Standard Model" section of this review.

8 Global Analysis of Electroweak Data

In presenting the status of combined electroweak fits, we have borrowed from work of the LEP Electroweak Working Group in Sections 8.1-8.4 . A more complete discussion of the data and of their fitting procedures can be found in their 1994 paper [38]. A more detailed review of LEP electroweak physics, including future prospects, is given in reference [92].

8.1 Lepton Universality

The most precise test of universality for the charged-current interaction comes from the ratio $R_{e/\mu} = , (\pi \to e\bar{\nu}_e)/, (\pi \to \mu\bar{\nu}_\mu)$. This ratio is not affected by the strong interactions to zeroth order in α; the $O(\alpha)$ corrections have been calculated to be $\approx$ 3.7%, and general arguments given in Refs. [93,94] indicate that the calculation is very precise. The ratio of experimental results [95] to theory [94] gives

$$\frac{R^{exp}_{e/\mu}}{R^{th}_{e/\mu}} = 0.9966 \pm 0.0030 \pm 0.0004, \qquad (34)$$

where the errors are experimental and theoretical, respectively. Alternatively, introducing effective $SU(2)_L$ couplings associated with the $(e\nu_e)$ and $(\mu\nu_\mu)$ currents, one obtains

$$\frac{g_e}{g_\mu} = 0.9983 \pm 0.0015 \pm 0.0002, \qquad (35)$$

which is an impressive verification of e-μ universality. As the amplitudes involved are proportional to the W four-momentum q^μ, this test probes the longitudinal W couplings, and constrains heavy neutrino mixing, possible contributions from additional charged Higgs scalars, leptoquarks, and compositeness [96].

The tau coupling ratio can be extracted from $Br(\tau \to e\bar{\nu}_e\nu_\tau(\gamma)) = \tau_\tau$, $(\tau \to e\bar{\nu}_e\nu_\tau(\gamma))$, giving

$$\left(\frac{g_\tau}{g_\mu}\right)^2 = Br(\tau \to e\bar{\nu}_e\nu_\tau(\gamma))\frac{\tau_\mu}{\tau_\tau}\left(\frac{m_\mu}{m_\tau}\right)^5 \times 0.9996 \qquad (36)$$

where g_τ and g_μ are again effective couplings associated with the $(\nu_\tau\tau)$ and $(\nu_\mu\mu)$ currents. Tau decays also provide a measurement of e-μ universality using

$$\left(\frac{g_\mu}{g_e}\right)^2 = \frac{Br(\tau \to \mu\bar{\nu}_\mu\nu_\tau(\gamma))}{Br(\tau \to e\bar{\nu}_e\nu_\tau(\gamma))} \times 1.02821, \qquad (37)$$

where the numerical factors in both equations reflect phase-space differences, radiative corrections, and propagator effects. Inserting the experimental values [96] gives

$$\frac{g_\tau}{g_\mu} = 0.9949 \pm 0.0064 \qquad (38)$$

$$\frac{g_\mu}{g_e} = 0.9983 \pm 0.0060 \qquad (39)$$

providing a very nice test of e-μ-τ universality for charged current couplings.

Universality of the neutral current couplings has been tested at LEP from the partial widths of the Z to each of the three lepton flavors (which primarily determines g_{A_ℓ} for each lepton l), and from the forward-backward asymmetries for each lepton flavor (giving g_{V_ℓ}), as presented in Section 4.1.2; tau polarization measurements, described in Section 4.1.3, have also been used to extract $\mathcal{A}_e$ and $\mathcal{A}_\tau$. A combined fit to the LEP lineshape, forward-backward asymmetries, and tau polarization data give the following ratios of leptonic coupling constants:

$$\begin{aligned} g_{A_\mu}/g_{A_e} &= 1.0014 \pm 0.0021\ , \\ g_{A_\tau}/g_{A_e} &= 1.0034 \pm 0.0023\ , \\ g_{V_\mu}/g_{V_e} &= 0.83 \quad \pm 0.16\ , \\ g_{V_\tau}/g_{V_e} &= 1.044 \pm 0.091\ . \end{aligned} \qquad (40)$$

The best-fit values of the couplings are presented and compared graphically in Figure 4.

8.2 The Invisible Width of the Z

About 20% of the Z decays are expected to be into $\nu\bar{\nu}$ final states, which cannot be directly observed. The invisible width of the Z can be experimentally measured using

$$\begin{aligned} \frac{, inv}{, \mu\mu} &= \frac{, Z - , had - 3 \times , ll}{, \mu\mu} \\ &= \sqrt{\frac{12\pi R_l}{M_Z^2\ \sigma^0_{had}}} - R_l - 3. \end{aligned} \qquad (41)$$

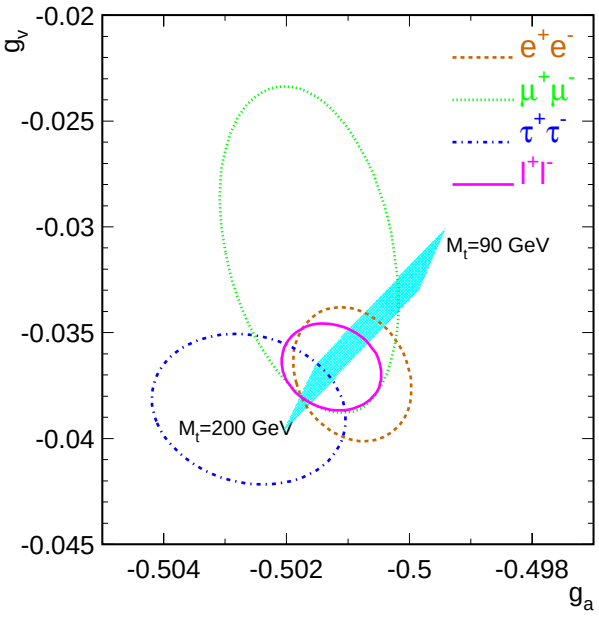

Figure 4: 68% probability contours in the g_{V_ℓ}-g_{A_ℓ} plane. The solid contour results from a fit assuming lepton universality. The shaded band represents the Standard Model prediction.

From this ratio and the expected SM couplings, one can calculate the number of light neutrinos to be [38]

$$N_\nu = 2.988 \pm 0.023 \qquad (42)$$

to be compared to an expected value of 3 (for 3 leptonic doublets). The ratio Γ_{inv}/Γ_{ll} is insensitive to α_s and to loop corrections (and therefore insensitive to M_t and M_H). This measurement is consequently an important test of the $SU(2)\times U(1)$ structure of the couplings of the leptonic doublets.

8.3 *The Effective Electroweak Mixing Angle* $\sin^2\theta_{\rm eff}$

If the universality of leptonic couplings, and the analogous universality of couplings for each of the three doublets of quarks is assumed, then the SM predicts the relative strengths of all of these couplings as a function of the single parameter $\sin^2\theta_{\rm W}^{eff}$. Therefore $\sin^2\theta_{\rm W}^{eff}$ can be measured independently in a number of different ways, as shown in Table 2. The comparison of these measurements provides a major test of the standard model, and in particular of the g_V and g_A structure of the couplings.

The first 6 lines of Table 2 are from the LEP experiments [38] and give a χ^2 of 2.8 for 5 degrees of freedom. The values of $\sin^2\theta_{\rm W}^{eff}$ obtained from lepton asymmetries, tau polarization ($\mathcal{A}_\tau$ and $\mathcal{A}_{\rm e}$ combined), and $A_{\rm FB}^{0,\,b}$ all give independent and consistent results, with similar precision.

The last line gives the SLC value of $\sin^2\theta_{\rm W}^{eff}$ from the measurement of A_{LR}, and differs by 2.4 σ from the average of the others. The ratio of the LEP and SLC quantities is not sensitive to higher-order loop corrections, and it is difficult to find any natural theoretical reason for a difference. SLC measurements should improve by a factor of two within the next few months. We assume in this report that the present small discrepancy will be resolved with better measurements; if this is not the case, understanding the reason for the difference will be crucial.

8.4 *Standard Model Fits to Electroweak Data (Not Including* M_t*)*

The Standard Model predicts the masses of the gauge bosons W and Z as a function of $\sin^2\theta_W$, as well as the magnitudes of the couplings. This allows precise comparisons of a number of independent measurements; their precision makes them sensitive to α_s, and to the masses M_t (top quark) and M_H (Higgs boson) through loop corrections. The leading top quark dependence is quadratic and allows a determination of M_t. The dependence on M_H is logarithmic, and consequently M_H cannot be reliably determined without a direct measurement of M_t.

The LEP Electroweak Group has combined LEP measurements using the full correlation matrix between the different measurements, and has simultaneously fitted M_t and α_s to the data under Standard Model assumptions. Table 3 shows the constraints obtained on M_t and $\alpha_s(M_Z^2)$ when fitting all electroweak measurements to Standard Model calculations. The fits have been repeated for $M_H = 60$, 300 and 1000 GeV and the difference in the fitted parameters is quoted as the second uncertainty in each parameter. The second column gives the results from fitting LEP data alone, the third column includes M_W measurements and neutrino data, and the fourth column includes A_{LR} from SLC. The χ^2 for all these fits is acceptable.

The LEP measurements of the partial widths and of the asymmetries are sensitive in varying degrees to α_s and M_t. The individual measurements (LEP averages) and their errors are summarized in Table 4(a), which also gives the final errors expected from LEP 1 (discussed in Section 4.1 above and used in Section 8.6 below), the Standard Model fit assuming M_H=300 GeV, and the pull of each measurement on the fit. The sensitivities of each of these values to α_s and M_t is shown in Figure 5.

The only measurements that show any significant deviation from the SM predictions are $R_b = \Gamma_b/\Gamma_{had}$ from LEP and $\sin^2\theta_{eff}$ from the SLC measurement of A_{LR}. R_b is about 2.2 σ high (favoring a lower top mass), and A_{LR} is about 2.4 σ high (favoring a higher top mass), as further discussed in Section 8.5. These deviations do not seem remarkable in view of the large number of measurements that are included in the fit. Moreover, there is a correlation between the measurements of R_b and R_c;

Table 2: (from Ref. [38]) Comparison of several determinations of $\sin^2\theta^{\rm lept}_{\it eff}$ from asymmetries. Averages are obtained as weighted averages assuming no correlations.

	$\sin^2\theta^{\rm lept}_{\it eff}$	average by group of observations	$\chi^2/(d.o.f.)$	cumulative average	$\chi^2/(d.o.f.)$
$A_{\rm FB}^{0,\,\ell}$	0.2311 ± 0.0009				
$\mathcal{A}_\tau$	0.2320 ± 0.0013				
$\mathcal{A}_{\rm e}$	0.2330 ± 0.0014	0.2317 ± 0.0007	1.4/2	0.2317 ± 0.0007	1.4/2
$A_{\rm FB}^{0,\,\rm b}$	0.2327 ± 0.0007				
$A_{\rm FB}^{0,\,\rm c}$	0.2310 ± 0.0021	0.2325 ± 0.0006	0.6/1	0.2321 ± 0.0005	2.8/4
$\langle Q_{\rm FB} \rangle$	0.2320 ± 0.0016	0.2320 ± 0.0016	–	0.2321 ± 0.0004	2.8/5
A_{LR} (SLC)	0.2294 ± 0.0010	0.2294 ± 0.0010	–	0.2317 ± 0.0004	9.0/6

Table 3: (from Ref. [38]) Results of fits to LEP and other data for M_t and $\alpha_s(M_Z^2)$, assuming the Standard Model with a single Higgs boson. No external constraint on $\alpha_s(M_Z^2)$ has been imposed. In the third column the combined data from $p\bar{p}$ and neutrino experiments is also included, and the fourth column gives the result when the SLD measurement of A_{LR} is added. The central values and the first errors quoted assume $M_H = 300$ GeV (not the best fit to M_H). The second errors correspond to the variation of the central value when varying M_H in the interval $60 \leq M_H\ [\rm GeV] \leq 1000$.

	LEP	LEP + M_W and ν data	LEP + M_W and ν data + A_{LR} from SLC
M_t (GeV)	$173^{+12\ +18}_{-13\ -20}$	$171^{+11\ +18}_{-12\ -19}$	$178^{+11\ +18}_{-11\ -19}$
$\alpha_s(M_Z^2)$	$0.126 \pm 0.005\ \pm 0.002$	$0.126 \pm 0.005\ \pm 0.002$	$0.125 \pm 0.005\ \pm 0.002$
$\chi^2/(d.o.f.)$	7.6/9	7.7/11	15/12
$\sin^2\theta^{\rm lept}_{\it eff}$	$0.2322 \pm 0.0004\ ^{+0.0001}_{-0.0002}$	$0.2323 \pm 0.0003\ ^{+0.0001}_{-0.0002}$	$0.2320 \pm 0.0003\ ^{+0.}_{-0.0002}$
$1 - M_W^2/M_Z^2$	$0.2249 \pm 0.0013\ ^{+0.0003}_{-0.0002}$	$0.2250 \pm 0.0013\ ^{+0.0003}_{-0.0002}$	$0.2242 \pm 0.0012\ ^{+0.0003}_{-0.0002}$
M_W (GeV)	$80.28 \pm 0.07\ ^{+0.01}_{-0.02}$	$80.27 \pm 0.06\ ^{+0.01}_{-0.01}$	$80.32 \pm 0.06\ ^{+0.01}_{-0.01}$

Table 4: Summary of measurements included in the combined analysis of Standard Model parameters. Section a) summarizes LEP averages, Section b) gives $\sin^2\theta^{\rm lept}_{eff}$ from the measurement of the left-right polarization asymmetry at SLC, c) gives $\sin^2_\theta$ from νN-scattering, d) gives M_W from hadron colliders, and e) gives the recent M_t measurement from CDF. The third column gives the anticipated future errors. These are the final results for LEP 1 (1996), SLC (1998), νN (1998), and Tevatron Run 1b (1996). LEP 2 results (1999) are not included. The Standard Model fit result in column 4 and the pulls in column 5 are derived from the fit to all data *except* M_t for a fixed value of $M_H = 300$ GeV.

	measurement and error in 1994	anticipated error in 1998	Standard Model fit	pull (1994)
a) LEP 1				
line-shape and				
lepton asymmetries:				
M_Z [GeV]	91.1888 ± 0.0044	± 0.0025	91.1887	0.0
$,_Z$ [GeV]	2.4974 ± 0.0038	± 0.0025	2.4973	0.0
$\sigma^0_{\rm h}$ [nb]	41.49 ± 0.12	± 0.06	41.437	0.4
R_ℓ	20.795 ± 0.040	± 0.025	20.786	0.2
$A^{0,\ell}_{\rm FB}$	0.0170 ± 0.0016	± 0.0010	0.0153	1.0
τ polarization:				
$\mathcal{A}_\tau$	0.143 ± 0.010	± 0.005	0.143	0.0
$\mathcal{A}_{\rm e}$	0.135 ± 0.011	± 0.006	0.143	-0.7
b and c quark results:				
$R_{\rm b} = ,_{\rm b\bar{b}}/,_{\rm had}$	0.2202 ± 0.0020	± 0.0014	0.2158	2.2
$R_{\rm c} = ,_{\rm c\bar{c}}/,_{\rm had}$	0.1583 ± 0.0098	± 0.0080	0.172	-1.4
$A^{0,\rm b}_{\rm FB}$	0.0967 ± 0.0038	± 0.0022	0.1002	-0.9
$A^{0,\rm c}_{\rm FB}$	0.0760 ± 0.0091	± 0.0060	0.0714	0.5
$q\bar{q}$ charge asymmetry:				
$\sin^2\theta^{\rm lept}_{eff}$ from $\langle Q_{\rm FB}\rangle$	0.2320 ± 0.0016	± 0.0016	0.2320	0.0
b) SLC				
$\sin^2\theta^{\rm lept}_{eff}$ from $\mathcal{A}_{\rm e}$	0.2294 ± 0.0010	± 0.00025	0.2320	-2.6
c) νN scattering				
$1 - M^2_W/M^2_Z(\nu N)$	0.2256 ± 0.0047	± 0.0032	0.2242	0.2
d) M_W from $p\bar{p}$				
M_W [GeV] (CDF, DØ, UA2)	80.23 ± 0.18	± 0.110	80.32	-0.5
e) M_t from Fermilab				
M_t from lepton+jet events	$174. \pm 16.$	$\pm 8.$	178.	$+0.2$

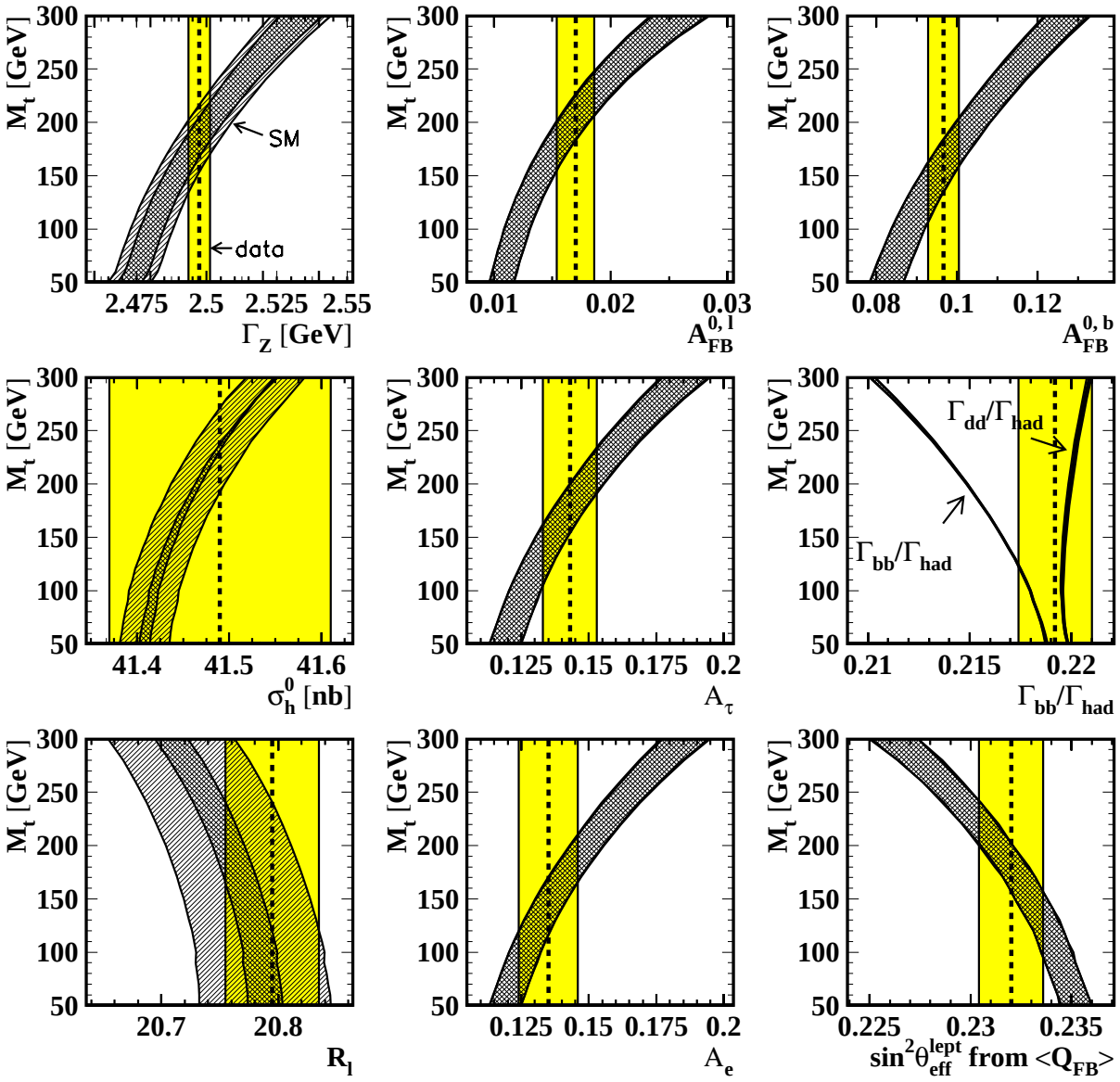

Figure 5: Comparison of LEP measurements with the Standard Model prediction as a function of M_t. The cross-hatched area shows the variation of the Standard Model prediction with M_H spanning the interval $60 < M_H\,(\mathrm{GeV}) < 1000$ and the singly-hatched area corresponds to a variation of $\alpha_s(M_Z^2)$ within the interval $\alpha_s(M_Z^2) = 0.123 \pm 0.006$. The total width of the band corresponds to the linear sum of both uncertainties. For the ratios of partial widths, $\Gamma_{b\bar{b}}/\Gamma_{had}$ and $\Gamma_{d\bar{d}}/\Gamma_{had}$, this variation nearly cancels. For the comparison of R_b with the Standard Model the value of R_c has been fixed to the Standard Model. The experimental errors on the parameters are indicated as vertical bands.

if R_c is fixed at its Standard Model value of 0.171, then the deviation of R_b is reduced to 1.9 σ. It is also worth noting that the electroweak corrections to R_b are different from all other electroweak corrections, since R_b is sensitive to the $W - t\bar{b}$ vertex. This quantity is therefore more sensitive to some kinds of deviations from the Standard Model. On the other hand, it is difficult to theoretically account for a difference between the values of $\sin^2\theta_{\rm eff}$ measured at LEP and SLC.

The internal consistency of all of these measurements, including R_b and A_{LR}, is very good. Moreover, the values of α_s and M_t obtained from these fits are consistent with external measurements of these parameters: event shape measurements at LEP give ($\alpha_s(M_Z^2) = 0.123 \pm 0.006$ [97]), and the top mass extracted by CDF from lepton+jet events is $M_t = 174 \pm 10^{+13}_{-12}$ GeV. This gives strong support to the idea that we are indeed seeing electroweak quantum corrections in the measured electroweak parameters, and that a massive top quark is a major source of these corrections. However, the remarkably close agreement between the predicted and measured values of M_t is of course fortuitous. One should note that the prediction given in Table 3 has assumed the fixed value $M_H = 300$ GeV; if M_H is left as a free parameter, a somewhat lower value of M_t is found as described below.

8.5 Comparison to Direct Measurements of M_W and M_t

As discussed in Section 2, the Standard Model is completely specified at tree level by the 3 parameters $\alpha(M_Z)$, G_F, and M_Z. When loop-level corrections are included, two additional parameters (*e.g.*, M_t and M_H) are required. It is convenient to choose the 2 parameters to be M_t and M_W, since the direct measurements of these masses are expected to improve very dramatically over the next decade.

Both M_t and M_W can be predicted from the e^+e^- and νN measurements listed in parts *a*), *b*), and *c*) of Table 4. The $M_t - M_W$ contours [98] from a Standard Model fit to this data (referred to below as "Z data", even though νN is also included) are compared to the direct measurements in Figure 6. The mass M_H of the Higgs (which can be calculated as a function of M_t, M_W, and the other SM parameters) is unconstrained in these fits. The shaded bands correspond to lines of constant M_H, with the width of the bands being due mainly to the uncertainty in $\alpha(M_Z)$. The best fit and the limits of the 1-σ contour, from the Z and νN data alone, correspond to the values $M_W = 80.315^{+0.066}_{-0.068}$ GeV and $M_t = 159.^{+18.}_{-15.}$ GeV. These values agree well with the direct measurements of M_W and M_t listed in Table 4 and displayed as the direct M_W-M_t point in Figure 6.

The shapes of the constraints from different measurements can be understood on an $M_t - M_W$ plot in terms of the leading order M_t and M_H dependence of the loop corrections. Since electroweak corrections involve two unknown parameters, any given measurement will produce a band in the $M_t - M_W$ plane; for example, the asymmetry measurements of $\sin^2\theta_{\rm eff}$ give a band which slopes upward slightly with increasing M_t. Both the size and the shape of the contours resulting from combining many measurements depend on the central values of those measurements, as well as on their errors. In particular, the contours of Figure 6 are significantly influenced by the two measurements which deviate from the best-fit SM values at the 2-σ level: these are R_b from LEP and A_{LR} from SLC. Figure 7 shows the 1-σ contour (shaded region) from the fit to all e^+e^- data *except* these two measurements, as well as the 1- and 2-σ contours from each of these measurements alone (the experimental constraints on M_Z and α_s are included in all contours).

The solid contour in the center of Figure 7 is determined mainly by the measurements of $\sin^2\theta_{eff}$ (giving a band with a slight upward slope to the right) and , $_Z$ (giving a wider roughly horizontal band). The intersection of these bands defines the solid contour. The SLC measurement of A_{LR} gives a band similar to the LEP $\sin^2\theta_{eff}$ band, but displaced upward due to the corresponding difference in $\sin^2\theta_{eff}$. The band from R_b has a very different dependence because of the strong $b - t$ coupling and the fact that the M_H dependence cancels in the ratio of , $_{b\bar{b}}$ to , $_Z$. Consequently R_b is virtually independent of M_H and gives an approximately vertical band in the figure between the limits imposed by the constraints on M_H.

As can be seen from Figure 7, the R_b data tend to pull M_t strongly to the left. The data A_{LR} contours, on the other hand, tend to pull almost vertically upward in M_W. The result of these two pulls is that M_t and M_H are both significantly pulled to lower values. The effects from these measurements, due to their deviation from SM predictions, contribute to the relatively small contours of Figure 6 and the relatively tight constraints on M_t, and especially on M_H.

If all measurements agreed precisely with the SM predictions, the contours would be somewhat larger. This is shown in Figure 8, in which the central values of all measurements have been shifted to the best fit using all the data of Table 4 (including M_W and M_t). Although Figure 6 unquestionably gives the more accurate picture of our present knowledge, it is impossible to predict how the contours will evolve in time since we do not know how the central values of individual measurements may change. Consequently we use the contours of Figure 8 as a reference point to gauge future improvements. When the measurements of LEP 1, LEP 2, SLC, νN, and Tevatron Run 2 are completed, the considerable reduction in errors should result in the contours shown in Figure 9

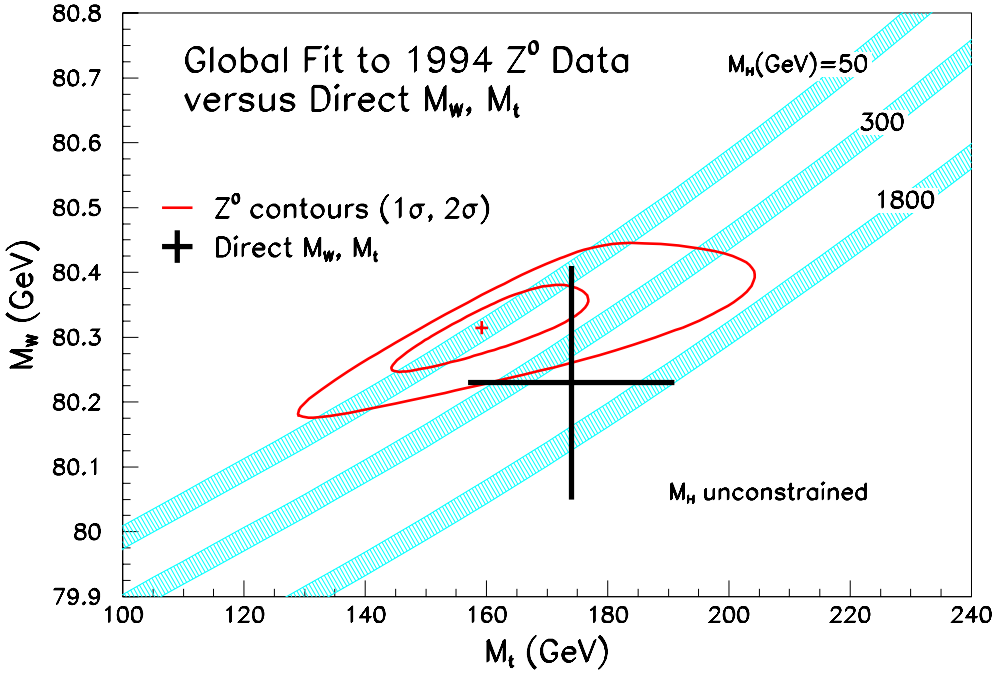

Figure 6: The $M_t - M_W$ contours from a global SM fit to all e^+e^- and νN data (parts a, b, and c of Table 4) are compared to the direct measurements. In the global fit, M_H is a free parameter; it ranges from 22 to 180 GeV on the 1-σ contour. The cross-hatched bands correspond to the indicated Higgs masses; the widths of the bands are due primarily to the uncertainty in $\alpha(M_Z)$.

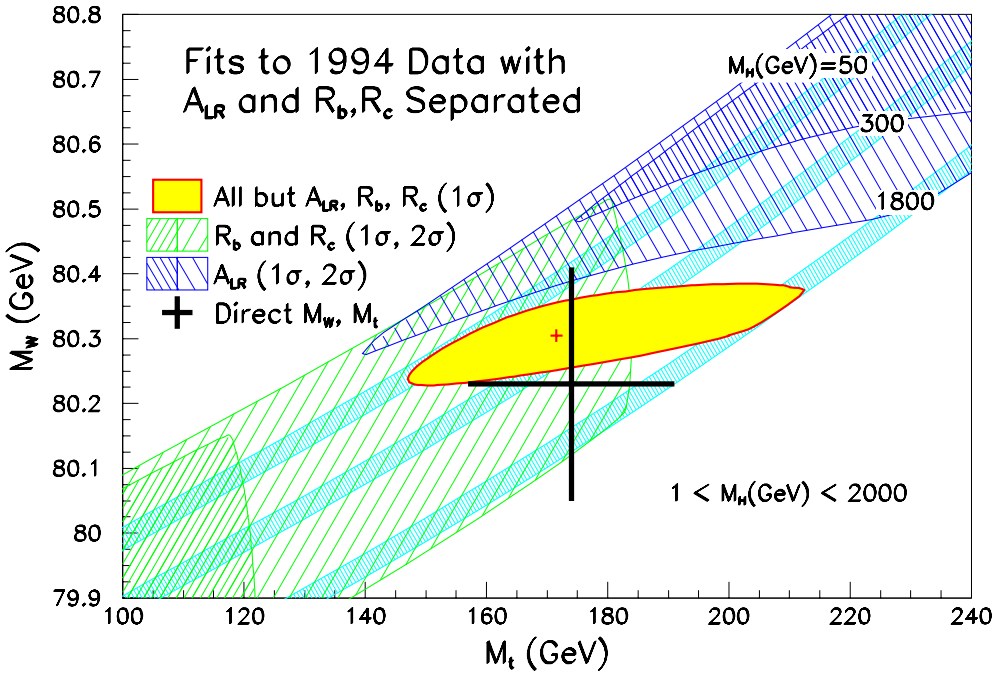

Figure 7: The 1- and 2-σ contours from A_{LR} measurements (upper right) and from R_b, R_c measurements (lower left) are separately displayed. All contours include the constraints from M_Z, $\alpha_s = 0.123 \pm 0.006$, and $1 < M_H(GeV) < 2000$. The solid contour in the center is the 1-σ limit from all other Z and νN data; M_H ranges on this contour from 37 GeV to the upper cutoff value of 2000 GeV.

(the specific resolutions assumed here are given in the following section). However, one should bear in mind that the actual contours in 2002 might look quite different, just as the "expected" contours of Figure 8 differ from the actual contours of Figure 6.

8.6 Future Expectations and Constraints on M_H

At the present time, electroweak measurements are in excellent agreement with the predictions of the Standard Model. Moreover, significant restrictions on the allowed Higgs mass are now just beginning to emerge from the data. Fortunately, major improvements in electroweak measurements are expected over the next decade, accompanied by major improvements in direct searches for the Higgs during the next two decades. The confrontation of the indirect determinations with the results of the direct searches will perhaps provide the ultimate test of the Standard Model. The precision of the predictions of M_H from electroweak data provides a useful benchmark of electroweak measurements, and is one indicator of which measurements are most important.

The sensitivity of the current Z_0 data alone to M_H is limited, since loop corrections are usually proportional to linear combinations of M_t^2/M_Z^2 and $\ln(M_H^2/M_Z^2)$, which are dominated by M_t. For this reason, an external measurement of M_t greatly improves the sensitivity to M_H. If the CDF determination of M_t from lepton+jet events is included in the full electroweak fit, then the sensitivity of the data matches the expectations from Monte-Carlo calculations and weakly favors a relatively low value of M_H. Reference [99] presents several ways of fitting all of the data, and obtains a best-fit Higgs mass in the range $50 < M_H < 130$ GeV in various fits, with an uncertainty on the order of a factor of two or three in each fit. The results vary by about a factor of two depending on the details of data treatment, as discussed in the paper. A similar fit by the LEP Electroweak Group [38] gives similar results.

However, we note that the resolution on the Higgs mass, in particular, is sensitive to the details of the fitting program as well as to the selection of input data. Moreover, the change in the value of $\alpha(M_Z)$ suggested by reference [33] would increase the central value of M_H by a factor of 3 or 4. The experimental evidence that the Higgs is light is not compelling at this time.

We defer to other work in progress [38,100] for more complete discussions of current data and analysis; in this report our emphasis is on the relative improvements to be expected from future data. Figure 10 shows how we expect the χ^2 curve for the Higgs mass to evolve in time as measurements improve. In producing this plot,[d] we have adjusted all measurements to agree with the Standard Model predictions for $M_H = 100$ GeV, and have then adjusted the errors of each measurement as a function of time in accordance with expectations, assuming that final results will lag behind data-taking by at least a year. At each step, we have examined the sensitivity of δM_H to a factor-of-two reduction in 5 sources of error: δM_t, δM_W, $\delta\alpha(M_Z)$, $\delta sin^2\theta_{eff}$ from all LEP and SLC measurements, and all other LEP measurements (M_Z, , $_Z$, σ_h^0, R, , $_{b\bar{b}}$, and , $_{c\bar{c}}$).

The major advances between now and 1996 come from the improvements in δM_t and δM_W from the Tevatron, in final LEP 1 measurements, and in $\mathcal{A}_e$ from SLC. The anticipated errors for both 1994 and 1996 are given in Table 4; we also assume a reduction in $\delta\alpha_s$ from 0.006 to 0.003 from LEP data (*e.g.*, event shapes, τ decays, etc.). The SLC error has been reduced to $\delta\sin^2\theta_{\rm eff}$=0.0005, and the Tevatron error on M_W has become 110 MeV. The biggest effect comes from the reduction of δM_t from 16 GeV to 8 GeV. The resulting uncertainty in M_H is reduced from $f_\sigma \approx$3.5 to $f_\sigma \approx 2.3$. At that point in time, δM_H will be most sensitive to improvements in δM_t and $\delta\alpha(M_Z)$.

Between 1996 and 1999, we expect a new measurement of $\sin^2\theta_W$ from the Fermilab neutrino experiment, and a reduction in the SLC error in $\sin^2\theta_{\rm eff}$ from 0.00040 to 0.00025, and a measurement of M_W from LEP 2 at a sensitivity of $\pm$50 MeV (preliminary LEP 2 errors). Since M_W will be predicted to a precision of 42 MeV from the LEP 1/SLC/νN data (31 MeV if M_t is included in the fit), this last measurement provides an impressive test of the Standard Model. There will be no new Tevatron collider results since Run 2 will only begin in 1998-9, and consequently there will be no reduction in δM_t. Since the uncertainty on M_H is still dominated by δM_t, the 1999 improvements do not give a major immediate improvement in δM_H although they will be important when δM_t is further reduced.

Between 1999 and 2002, we expect results from 1 fb^{-1} from Tevatron Run 2 and final results from LEP 2, giving errors of 40 MeV on M_W and 4 GeV on M_t; the resulting error on M_H is reduced to $f_\sigma \approx 2.0$.

During the first two or three years of LHC running, we assume a reduction on δM_t from 4 GeV to 2 GeV. No other improvements are assumed.

At this point in time (taken to be 2006) the error on M_H has been reduced to $f_\sigma \approx$1.9, and is most sensitive to improvements in M_W and $\alpha(M_Z)$; improvements in other measurements are relatively unimportant. Both M_W and

[d] Note that the horizontal scale in Figure 10 is logarithmic, and that the χ^2 curve appears to be parabolic in shape as a function of $\ln(M_H)$. This is because the loop diagrams contribute terms proportion to $\ln(M_H^2)$. As a consequence, the 1-σ deviations from M_H scale approximately with M_H, and it is better to quote the errors on M_H as a factor f_σ rather than as an absolute number. For example, in 1996 the 1-σ limits for 1996 are 40 and 225 GeV for M_H^0=100 GeV ($f_\sigma = 2.3$); these would be 85 and 409 GeV for M_H^0=200 GeV ($f_\sigma = 2.2$).

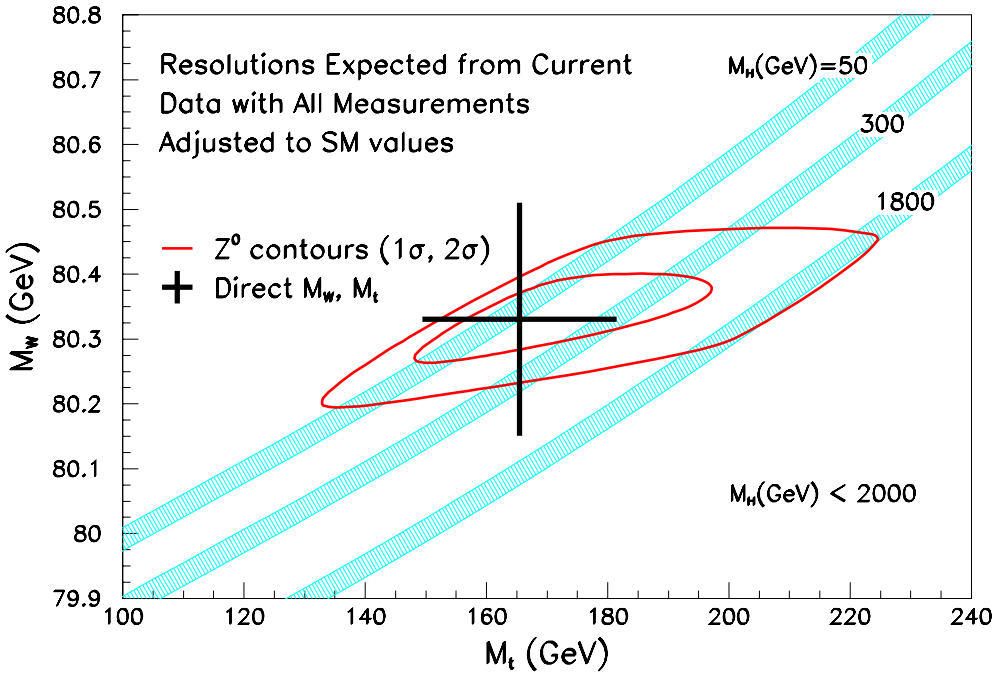

Figure 8: If the central values of all current measurements are shifted to agree with the predictions of the best-fit Standard Model, but with the correct current uncertainties as given in the left-most column of Table 4, then the contours of Figure 6 become the contours shown above.

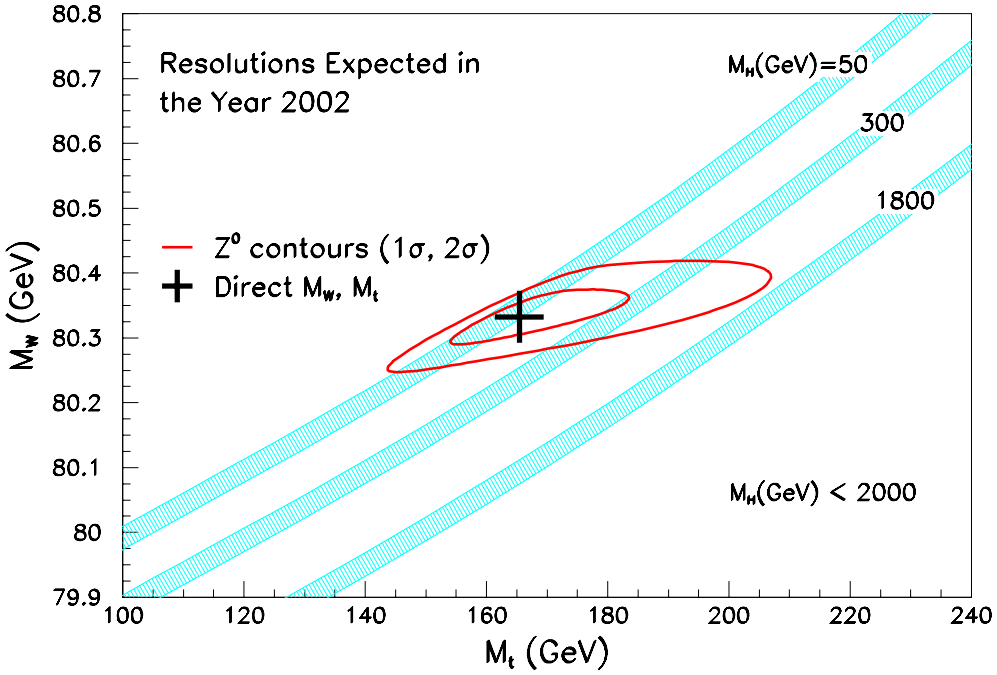

Figure 9: In calculating the EW contours from measurements other than M_t and M_W, the errors of all measurements have been reduced to be those that we anticipate after completion of the SLC, LEP 1, and Fermilab νN programs ($\sim$1998). The uncertainties in the direct measurements are taken to be $\delta M_W = 40$ MeV and $\delta M_t = 4$ GeV ($\sim$2002).

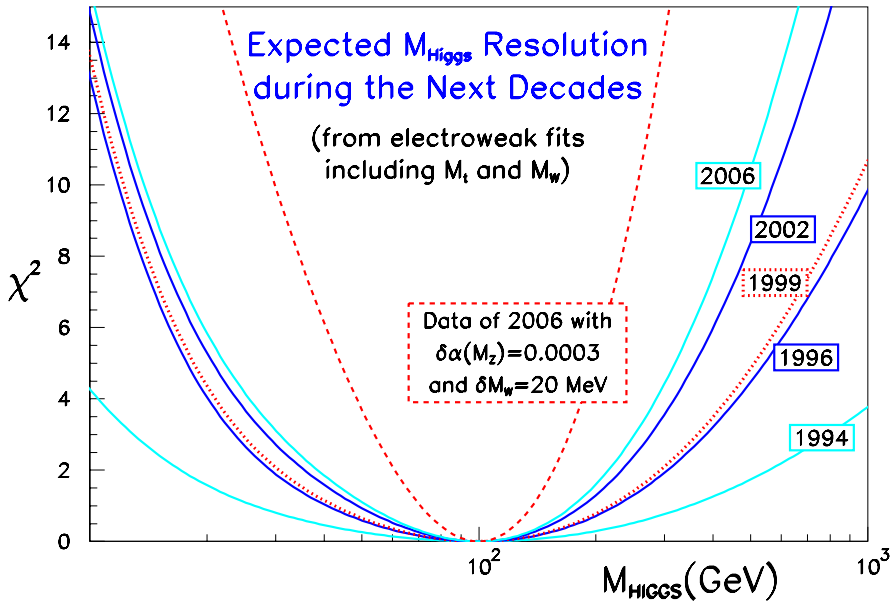

Figure 10: Anticipated sensitivity of the χ^2 curve from SM fits to the Higgs mass assuming $M_H = 100$ GeV, given as a function of time during the next decade. The inner-most (dashed) curve shows the effect of improving the measurements of both $\alpha(M_Z)$ and M_W beyond current expectations.

$\alpha(M_Z)$ are accessible to improved measurements, and we believe these should be a focus for additional work during the period 1994-2006.

Improvements in M_W might be possible at LEP 2 before LHC turns on, and at either LHC or the Tevatron after that. A reduction in δM_W from 40 to 20 MeV is certainly not easy to accomplish, but it might be attainable; indeed, the δM_W error of 40 MeV we have assumed for 2002 is probably somewhat pessimistic.

Similarly, during the latter half of the present decade, measurements at Novosibirsk, Daphne, Beijing, possibly Cornell, and perhaps other accelerators, combined with theoretical work, could lead to a reduction in the error on $\alpha(M_Z)$ of a factor of 2 or more; we believe this effort needs increased emphasis from both experimenters and theorists. As the final step in the evolution of Higgs resolution, we have assumed errors of $\delta M_W = 20$ MeV and $\delta\alpha(M_Z) = 0.0003$; these are to be taken as proposed goals rather than as projections.

If these improvements in both $\alpha(M_Z)$ and M_W are achieved, the resulting Higgs sensitivity is shown in the inner-most curve of Figure 10, and corresponds to an uncertainty in the Higgs mass of $f_\sigma \approx 1.4$. δM_H will not be dominated by any one measurement, and in fact its sensitivity to factor-of-two improvements in each of the five quantities considered is about the same. If M_H differs from 100 GeV, then the minimum of the χ^2 curves is shifted and the details of the shapes also change, but the general features of the curves are the same. In all of this analysis, we have ignored possible theoretical uncertainties in higher-order diagrams, including those in the $t-b$ vertex, in the expectation that theory will keep pace with experiments during this time.

The comparison between Z contours and direct measurements of M_t and M_W after these improvements is shown in Figure 11. The comparison of this figure to Figure 9 shows the effects of $\delta\alpha(M_Z)$ on both the contours and the widths of the Higgs bands, and also shows the factor-of-two improvements in the direct measurements of both M_t (from LHC) and M_W.

9 Direct Searches for the Higgs Boson

Future searches for the Higgs boson for other electroweak symmetry-breaking phenomena are discussed in more detail by the "Beyond the Standard Model" section of this report. But because of the importance of the comparison of the M_H predictions from precision experiments with the direct searches for the Higgs, we will briefly review here the expectations for Higgs searches over the next 15 years.

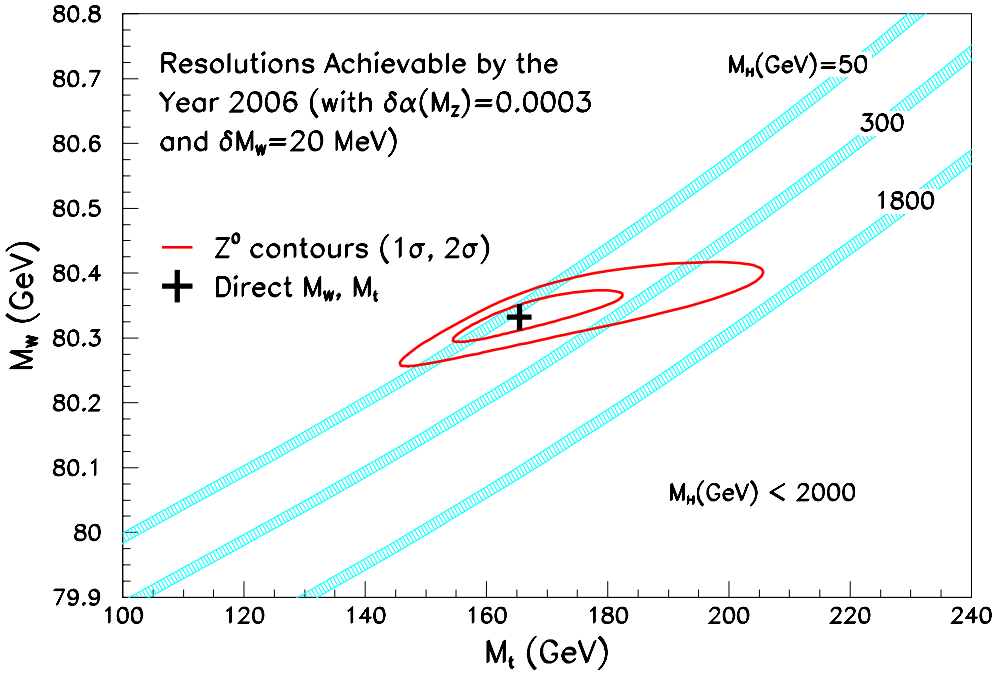

Figure 11: The electroweak contours here are calculated from the same data as in Figure 9, but with the error in $\alpha(M_Z)$ reduced by a factor of 3 to ± 0.0003. The uncertainties in the direct measurements are taken to be $\delta M_W = 20$ MeV and $\delta M_t = 2$ GeV (from LHC). Each of these 3 errors is felt to be perhaps optimistic, but nevertheless feasible.

9.1 Low Mass Region: $M_H < 100$ GeV

The best limits on the Higgs mass now come from the LEP experiments. The Higgs boson would be produced near the Z resonance through the reaction

$$e^+e^- \rightarrow Z \rightarrow Z^* + H, \qquad (43)$$

where Z^* denotes an off-mass-shell Z. Such events can be detected if the Z^* decays into l^+l^- or $\nu\bar{\nu}$. In the former mode, events are identified by the acoplanar l^+l^- (where $l = e$ or μ), and in the latter by the significant missing energy and transverse momentum of the event. In both modes, searches can be sensitive to inclusive hadronic decays of the Higgs.

All four of the LEP experiments have searched for such events in both of these modes (and others). No signal has been observed, and present lower limits from each experiment lie in the range of 55 to 60 GeV. Combining all of the four LEP searches gives a LEP limit of $M_H > 62.5$ GeV [101]. The experiments are seeing some events, consistent with the expectations from background, so it is unlikely that there will be a significant improvement in 1995-6.

The predominant production diagram for a Higgs at LEP 2 would be

$$e^+e^- \rightarrow Z^* \rightarrow Z + H \qquad (44)$$

similar to the LEP 1 production diagram except now it is the intermediate Z which is off-mass-shell.

The threshold for this production mechanism is $M_H + M_Z$, and the cross section rises fairly steeply above threshold. For a luminosity of 400 pb^{-1}, the 5-σ discovery limit for a single experiment for $E_{cm} = 175$ GeV is 82 GeV, and for $E_{cm} = 190$ GeV it is 92 GeV [102]. At the present time, it appears that the LEP 2 energy will be approximately $E_{cm} = 180$ GeV, corresponding to a Higgs limit of approximately 86 GeV. $E_{cm} = 196$ GeV could be attained with construction of additional RF cavities, extending the Higgs range up to 95-100 GeV. An integrated luminosity of 400 pb^{-1} or more appears feasible under either scenario.

9.2 High Mass Region: $M_H > 130$ GeV

It appears that this region will be covered adequately by the LHC. The decays $H \rightarrow ZZ$ and $H \rightarrow ZZ^*$, with both Z's decaying into lepton pairs (e^+e^- or $\mu^+\mu^-$), provide a clear signature and sufficient rate for Higgs masses up to 800 GeV. Both ATLAS and CMS calculate good sensitivities over the region $130 < M_H < 800$ GeV, and conclude that a Higgs with $130 < M_H(\text{GeV}) < 500$ can be discovered with 10 fb^{-1}, and that 100 fb^{-1} (1 year at design luminosity) would extend this range up to 800 GeV [77,78]. Other decay modes such as $ll\nu\nu$ and $lljj$

could extend this range up to 1 TeV with additional running.

The lower limit of this range is set by the branching ratio into ZZ^*, which falls off rapidly due to the Z^* propagator as M_H falls below about 130 GeV.

9.3 Intermediate Mass Region: $85 < M_H < 130$ *GeV*

This region, between the LEP 2 limit and the region of significant branching ratio for $H \to ZZ^*$, is experimentally the most difficult one to cover. Unfortunately, there are both theoretical and experimental reasons to suspect that this may be one of the most interesting regions.

LEP 2 will cover the lower part of this region, up to a limit of perhaps 80-90 GeV. The LHC, and possibly the Fermilab collider after luminosity upgrades, will have some sensitivity. But the dominant decay mode $H \to b\bar{b}$ does not allow precise mass reconstruction and may be swamped by hadronic backgrounds in hadron colliders. The two final states which appear to offer the best opportunity for a discovery of the Higgs in this mass region are discussed below:

9.3.1 $H \to \gamma\gamma$

In the intermediate mass range ($80 < M_H < 130$ GeV) the decay $H \to \gamma\gamma$ gives the best signature for Higgs detection, in spite of a low branching ratio ($\sim 0.1\%$). Good mass resolution on the Higgs requires measurement of the γ angles as well as their energies, and backgrounds are severe.

Both ATLAS and CMS have calculated their expected sensitivity to a Higgs in this mass region [77,78], and each estimates a sensitivity $S/\sqrt{B} \geq 5$ for $90 \leq M_H \leq 150$ GeV (S=signal, B=background). However, the sensitivities depend critically on calorimeter performance and pile-up effects. Better estimates should be available soon in the Technical Design Reports of each detector, which will include improved calorimeter design parameters.

However, even if the LHC detectors can adequately cover this decay mode, the Higgs sensitivity would still be quite sensitive to the $\gamma\gamma$ branching ratio, which would be reduced in some modest extensions to the Standard Model, including the minimal supersymmetric model. This could make detection of the Higgs by its $\gamma\gamma$ decay impossible at the LHC. In any case, one would certainly put a high priority on the detection of the dominant decay modes of the Higgs, and on the measurement of its branching ratios.

9.3.2 WH Production, with $W \to l\nu$ and $H \to b\bar{b}$

Several groups [103,104,105] have recently investigated the possibility of detecting the $H \to b\bar{b}$ decay, with the Higgs produced via WH or ZH production and using the leptonic decays of the gauge bosons as an additional tag to reduce backgrounds. Tagging of each of the b's is essential, as are kinematic cuts to suppress $t\bar{t}$ backgrounds. Estimates of $S/\sqrt{B}$ range from about 4.8 to 6.6 for a 100-GeV Higgs with 30 fb^{-1} of data, with improved sensitivity for a lower mass Higgs.

Both references [103,104] have found that, for equal luminosities of 30 fb^{-1}, Fermilab and LHC have similar sensitivities to this mode; the signal is larger at the LHC, but so are the backgrounds. The required luminosity would correspond to one or two years of low-luminosity running at the LHC, and probably a longer period of running at full luminosity at an upgraded Tevatron (TeV*). It is not clear that experiments at either accelerator could carry out the b-tagging and reconstruction necessary to identify these events, since rates and multiple-interaction problems will be severe. Because backgrounds are quite different between these two machines, further studies of both possibilities are needed.

9.4 Higgs Physics at the NLC

At a 500 GeV linear collider, the Standard Model Higgs boson would be produced by WW fusion and Z bremsstrahlung ($e^+e^- \to \nu\bar{\nu}H, ZH$). The primary sources of background are the processes: $e^+e^- \to W^+W^-$, $e^+e^- \to q\bar{q}$, and $e^+e^- \to e\nu W$. A data sample corresponding to one year of operation at design luminosity (50 fb^{-1}) would contain about 200 reconstructed ZH events in the 4-q, 2-q2-ℓ, and 4-ℓ channels if the Higgs mass is 150 GeV. Beam energy and Z mass constraints enhance the resolution of the kinematic event reconstruction and permit the isolation of reasonably pure event samples (the background to the 4-q sample is about 20%). A 50 fb^{-1} sample would permit the observation of a significant signal (5σ) up to a Higgs mass of 300 GeV [106].

Within the mass reach of the machine (a 1 TeV collider would have about twice the mass reach), a number of Higgs properties can be determined. The large signal-to-noise ratio enables the precise measurement of the Higgs mass (a resolution of 180 MeV is possible at a Higgs mass of 110 GeV) and the determination of the Higgs spin and CP parity. The measurement of the cross section for $e^+e^- \to ZH \to \ell^+\ell^- H$ with a 50 fb^{-1} sample would determine the ZHH couplings with a statistical precision of about 8% at $M_H = 110$ GeV. In the region $M_H < 2M_W$, the Higgs branching ratios to $b\bar{b}$, $c\bar{c} + gg$, $\tau^+\tau^-$, and WW^* can be measured (the precisions for $M_H = 110$ GeV are: 7%, 40%, 15%, and 50%, respectively [107]).

Since the Standard Model Higgs boson is not necessarily the most likely source of spontaneous symmetry breaking, we note that non-standard Higgs states (including composite ones and those that decay into invisi-

ble particles) can also be observed and studied at a linear collider (see the Spontaneous Symmetry Breaking Working Group section).

10 Couplings of the Gauge Bosons

The standard electroweak model is based on non-abelian gauge groups and as such makes clear predictions about the mutual couplings of the gauge bosons, γ, W and Z. These couplings can be related to the static or transition moments of those particles. The measurement of these couplings represents a program not unlike that of measuring g_A and g_V for the fermions. Initially one tests the basic structure. Eventually, with sufficient precision in the measurements, there is sensitivity to other sectors of the theory, for example the Higgs structure.

While there are some low energy experiments with indirect sensitivity [108] to the values of these couplings, much more direct measures are afforded in high-energy experiments when pairs of bosons, $W\gamma$, WW, WZ, $Z\gamma$ and ZZ are kinematically allowed. Several new results have been recently presented [109] from the Tevatron experiments. As an example, the current limits on the parameter $\Delta\kappa_\gamma$ related to the anomalous magnetic moment of the W can be expressed as $-2.3 \leq \Delta\kappa_\gamma \leq 2.2$ from either the CDF or DØ experiments [110]: $\Delta\kappa_\gamma = 0$ is the standard model value.

With 1 fb^{-1}, the limits are expected to reduce by an order of magnitude. Similar sensitivity is expected at LEP 2; the correlations between the couplings are different between e^+e^- and $p\bar{p}$ processes and this affects the sensitivities to different couplings.

At LHC with much higher energy and with an integrated luminosity of 100 fb^{-1}, approximately two orders of magnitude reduction in the bounds would be realised, assuming standard behavior. This achieves the level of sensitivity at which different extensions of the standard model suggest observable effects. Similarly, at an e^+e^- linear collider with 500 GeV in the center of mass, the limits offered are $-0.0024 \leq \Delta\kappa_\gamma \leq 0.0024$.

The reader is referred to the section prepared by the Electroweak Symmetry Breaking subgroup for more details.

11 Conclusions

Precision electroweak measurements from LEP, SLC, and Fermilab now provide stringent tests of the Standard Model. A dramatic test of the SM is given by the comparison of the mass of the top quark predicted from precision measurements of M_W and electroweak couplings with a direct measurement from hadron collider experiments. Evidence for a top quark of the expected mass has been presented by CDF this year. During the next decade, there will be a number of other major improvements in measurements of M_W, M_t, and electroweak couplings. These measurements provide important tests of the Standard Model and will give significant constraints on the mass of the Higgs boson. The confrontation of these indirect predictions of M_H with the results of direct searches for the Higgs will be perhaps the most exciting development of the next two decades in the field of particle physics.

In this report, we have reviewed the status of all the major electroweak measurements, including precision measurements of electroweak couplings and of the masses M_W and M_t, and have attempted to project the resolutions that will be attained in each measurement as a function of time over the next 15 years. We have examined how these improved measurements will affect tests of the Standard Model, and how the resolution on the predicted mass of the Higgs boson is expected to evolve during this time. We have also briefly reviewed the status and expectations of direct searches for the Higgs at LEP and LHC.

In general, we believe the presently planned program of electroweak measurements is an excellent one. It requires completion of the current programs at LEP 1, SLC, and Fermilab (Run 1b), followed by major new measurements at LEP 2, Fermilab (Run 2), and the LHC.

We believe there are three ways in which the present program might be improved:

- The accurate measurement of M_t is a key element in electroweak tests, and consequently the accumulation of high statistics during the present Tevatron Run 1b is of prime importance; after this run, there will be no new information on M_t for about 5 years. An accurate knowledge of M_t and the consequent improvement in predictions of M_H may be important for future planning during that time. We believe it is crucial to establish the observation of the top quark beyond any doubt, and highly desirable to improve the mass resolution to the level of $\sim$8 GeV during Run 1b. This might require up to 200 pb^{-1} of integrated luminosity.
- As measurements at LEP and SLC continue to improve, the uncertainty in $\alpha(M_Z)$ will become an increasing limitation in the precision of electroweak tests. The determination of this quantity is limited by the knowledge of the γ–hadron coupling at low q^2, needed for the evaluation of radiative corrections to $\alpha(M_Z)$. We believe there needs to be an increased emphasis on overcoming the experimental and theoretical limitations in determining $\alpha(M_Z)$, and reducing the error on this quantity by a factor of three (to ± 0.0003).
- The other parameter which will have the most significant effect on the ultimate precision of electroweak tests, and on the predictions of the mass of the Higgs

boson, is M_W. It appears that a resolution of 40 MeV is achievable under the the current program, – but an improved resolution of 20 MeV is desirable, and would give a better match to other resolutions. This improvement is difficult to attain, but it can be addressed at a number of different accelerators: LEP 2, the Tevatron, the LHC, and the NLC. The possibilities for improvements in these measurements should be more thoroughly explored.

With regard to direct searches for the Higgs boson and for the origin of electroweak symmetry breaking, we believe the situation is not altogether satisfactory. Data taken at LEP 2 and LHC will extend the region of sensitivity enormously, and are likely to lead to the discovery of the Higgs if the Standard Model is indeed correct. However, coverage of the low-mass region at the LHC (from 80 to 130 GeV) is predominantly from the $\gamma\gamma$ decay mode, and complete coverage is a significant challenge. Every effort must be made to avoid a hole in Higgs coverage between LEP 2 and LHC. In addition, detection of other (dominant) decay modes should be a priority. The LHC and LEP 2 physicists are addressing these problems, and we will have a better understanding of the experimental limitations at both facilities within the next year.

Some studies have indicated that the Fermilab Tevatron, with major upgrades in luminosity and perhaps energy, could be sensitive to a Higgs in this mass region. More detailed studies of the physics potential of an upgraded Tevatron, and of anticipated detector resolutions and overall performance, should be emphasized during the next two years. In conjunction with this, studies of necessary upgrades to both the experiments and the accelerator should be carried out.

Acknowledgements

While the conveners of the Working Group take responsibility for the contents of this report, they were helped in its production by many others. These contributed either through private communications, verbal or written, or comments on some draft. In addition some groups met to discuss specific issues such as the projection of the top mass measurement error, the W mass measurement error, and the tri-boson couplings. The LEP Electroweak Working Group at CERN was especially helpful, and made many of their results available to us ahead of publication. We are grateful for all the help received, and want to particularly acknowledge the following contributors:

H. Aihara, D. Amidei, D. Baden, T. Barklow, U. Baur, R. Bernstein, E. Blucher, R. Brock, D. Burke, W. Carithers, P. Clarke, M. Della Negra, M. Demarteau, S. Errede, T. Ferbel, H. E. Fisk, L. Foa, A. Galtieri, H. Frisch, N. Hadley, U. Heintz, C. Hill, I. Hinchliffe, P.Grannis, G. Kane, Young Kee Kim, B. Klima, S. Kopp, A. Liss, G. Mikenberg, M. Narain, L. Nodulman, L. S. Orozco, M. Pang, S. Parke, M. Peskin, C. Quigg, R. Raja, J. Rosner, D. Saltzberg, D. Schaile, D. Schlatter, M. Shochet, M. Strovink, J. Thompson, C. Wieman, C. Wendt, B. Winer, D. Wood, and C. Wyss.

References

[1] A. Sirlin, "The Standard Electroweak Model circa 1994: a Brief Overview," *Comments Nucl. Part. Phys.* **21**, 287 (1994).

[2] CDF Collaboration: F.Abe *et al.*, *Phys. Rev. Lett.* **73** (1994) 225;
F.Abe *et al.*, Fermilab PUB-94/097-E(1994), *Phys. Rev. D* **50**, 2966 (1994).

[3] D. Schaile and P.M. Zerwas, *Phys. Rev. D* **45**, 3262 (1992).

[4] C. Bouchiat, J. Iliopoulos, and P. Meyer, *Phys. Lett. B* **38**, 519 (1972).

[5] W.J. Marciano, *Radiative Corrections to Neutral Current Processes,* to appear in "Precision Tests of the Standard Electroweak Model," Advanced Series in High Energy Physics, World Scientific Publishing Co., P. Langacker, editor.

[6] M. Sher, *Phys. Lett. B* 317, 159 (1993) and Addendum; G. Altarelli, Electroweak Summary Talk at the Tennessee International Symposium on "Radiative Corrections: Status and Outlook", Gatlinburg, Tennessee, June 27-July 1, 1994.

[7] E. Farhi and L. Susskind, *Phys. Rep.* **74**, 277 (1981); M. Peskin and T. Takeuchi, *Phys. Rev. D* **46**, 381(1992).

[8] W. Marciano, *Phys. Rev. D* 41, 219(1990); W. Bardeen, C. Hill, and M. Lindner, *Phys. Rev. D* **41**, 1647 (1990).

[9] For a review, see J.F. Gunion *et al.*, "The Higgs Hunters Guide", Addison-Wesley, Redwood City, 1990.

[10] P. Langacker and M. Luo, *Phys. Rev. D* 44, 817 (1991); U. Amaldi, W. de Boer, and H. Furstenau, *Phys. Lett. B* **249**, 441 (1990); A. Sirlin, *Phys. Lett. B* **232**, 123 (1989).

[11] Particle Data Group, L. Montanet *et al.*, *Phys. Rev. D* **50**, 1173, (1994).

[12] A. Sirlin, *Phys. Rev. D* **22**, 971 (1980); ibid. **29**, 89 (1984).

[13] A. Sirlin, *Phys. Lett. B* 232, 123 (1989); G. Degrassi, S. Fanchiotti, and A. Sirlin, *Nucl. Phys. B* **351**, 49 (1991).

[14] M. Veltman, *Nucl. Phys. B* **123**, 89 (1977).

[15] W. Marciano and A. Sirlin, *Phys. Rev. D* **22**, 2695 (1980); G. Degrassi and A. Sirlin, *Nucl. Phys. B* **352**, 342 (1991).

[16] R. Barbieri *et al.*, *Phys. Lett. B* **288**, 95 (1992); J. Fleischer, O.V. Tarasov, and F. Jegerlehner, BI-TP-93/24, PSI-PR-93-14.

[17] A. Djouadi and C. Verzegnassi, *Phys. Lett. B* **195**, 265 (1987); A. Djouadi, *Nuovo Cimento A* **100**, 357.

[18] J. Fleischer *et al.*, *Phys. Lett. B* **293**, 437 (1992); G. Degrassi, *Nucl. Phys. B* **407**, 271 (1993); G. Buchalla and A.J. Buras, MPI-PTh111-92, TUM-T31-36/92 (1992).

[19] P. Gambino and A. Sirlin, *Phys. Rev. D* **49**, R1160 (1994).

[20] A. Sirlin, "Universality of the Weak Interactions," to appear in Precision Tests of the Standard Electroweak Model, Advanced Series in high-energy Physics, ed. P. Langacker (World Scientific); A. Sirlin, *Nucl. Phys. B* **71**, 29 (1974); A. Sirlin, *Rev. Mod. Phys.* **50**, 573 (1978).

[21] P. Gambino and A. Sirlin, *Phys. Rev. Lett.* **73**, 621 (1994)..

[22] M. Peskin and T. Takeuchi, *Phys. Rev. Lett.* **65**, 964 (1990); M. Golden and L. Randall, *Nucl. Phys. B* **361**, 3 (1991); W. Marciano and J. Rosner, *Phys. Rev. Lett.* **65**, 2963 (1990); D. Kennedy and P. Langacker, *Phys. Rev. Lett.* **65**, 2967 (1990); B. Holdom and J. Terning, *Phys. Lett. B* **247**, 88 (1990).

[23] See, for example, the second paper in Ref. [6].

[24] P. Langacker, talk presented at the Tennessee International Symposium on "Radiative Corrections: Status and Outlook," Gatlinburg, Tennessee, June 27 - July 1, 1994.

[25] G. Altarelli, R. Barbieri, and S. Jadach, *Nucl. Phys. B* **369**, 3 (1992); G. Altarelli, R. Barbieri, and F. Caravaglios, *Nucl. Phys. B* **405**, 3 (1993).

[26] W.J. Marciano, Lectures given at the 1993 SLAC Summer Institute, BNL-60177.

[27] G.L. Kane, in Proceedings of the International Workshop on Supersymmetry and Unification of Fundamental Interactions, ed. P. Nath (World Scientific, Singapore, 1993) p. 209.

[28] We would like to thank I. Hinchliffe, F. Jegerlehner, M. Peskin and C.Quigg for helpful discussions on this issue.

[29] G. Degrassi, S. Fanchiotti and A. Sirlin, *Nucl. Phys. B* **351** (1991) 49.

[30] F. Jegerlehner, *Z. Phys. C* **32** 195, (1986).

[31] H. Burkhardt, F. Jegerlehner, G. Penso and C. Verzegnassi, *Z. Phys. C* **43**, 497, (1989).

[32] J. Thompson, Private Communication.

[33] Morris L. Swartz, *Reevaluation of the Hadronic Contributions to* $\alpha(M_Z^2)$, SLAC-PUB-6710, November 1994.

[34] S. Eidelman and F. Jergerlehner, *Hadronic Contribution to g-2 of the Leptons and to the Effective Fine Structure Constant* $\alpha(M_Z^2)$, PSI-PR-95-1, January 1995.

[35] ICFA Workshop on Linear Colliders; Saariselka, Finland, September 1991; ed. R. Orava, P. Eerola, and M. Nordberg. World Scientific, 1993.

[36] Physics and Experiments with Linear e^+e^- Colliders; Hawaii, 1993; pp 141-165, ed. F.A.Harris, S.L.Olsen, S.Pakvasa, X. Tata; World Scientific, 1993.

[37] L. Arnaudon *et al.*, (LEP Energy Working Group), *Accurate Determination of the LEP Beam Energy by Resonant Depolarization*, CERN-SL/94-71 (BI), August 1994.

[38] *Combined Preliminary Data on Z Parameters from the LEP Experiments and Constraints on the Standard Model*, by the LEP Collaborations and the LEP Electroweak Working Group; CERN/PPE/94-187, 25 November 1994 (prepared from contributions of the LEP experiments to the *27th International Conference on High Energy Physics*, Glasgow, Scotland, 20-27 July 1994).

[39] LEP Electroweak Working Group, *LEP Electroweak Heavy Flavour Results for Summer 1994 Conferences*, LEPHF/94-03, ALEPH Note 94-119 PHYSIC 94-103, DELPHI 94-108 PHYS 425, L3 Note 1630, OPAL Technical Note TN242.

[40] SLD Collaboration, K. Abe *et al.*, SLAC-PUB-6456, March 1994, submitted to *Phys. Rev. Lett.* .

[41] P. Langacker, M. Luo, A. Mann, *Rev. Mod. Phys.* **64**, 87 (1992).

[42] J.V. Allaby *et al.*, *Z. Phys. C* **36**, 611 (1987).

[43] A. Blondel *et al.*, (CDHS Collaboration), *Z. Phys. C* **45**, 361 (1990).

[44] CCFR Collaboration, *Phys. Rev. Lett.* **72**, 3452 (1994).

[45] CCFR Collaboration, *Phys. Rev. Lett.* **70**, 134 (1993).

[46] P. Vilain *et al.*, *Precision Measurement of Electroweak Parameters from the Scattering of Muon-Neutrinos on Electrons*, CERN-PPE/94-124, June 30, 1994.

[47] W.J. Marciano and J.L. Rosner, *Phys. Rev. Lett.* **65**, 2963 (1990) and P.G.H. Sandars, *J. Phys. B* **23**, L655 (1990).

[48] M. Swartz, private communication.

[49] M.C. Noecker, B.P. Masterson, and C.E. Wieman, *Phys. Rev. Lett.* **61**, 310 (1988).

[50] M.A. Blundell, W.R. Johnson, and J. Sapirstein *Phys. Rev. Lett.* **65**, 1411 (1988).

[51] B.W. Lynn and P.H. Sandars, SSCL-Preprint-183, June 1993.

[52] D.M. Meekof, *et al.*, *Phys. Rev. Lett.* **71**, 3442 (1994); D.M. Meekof, *et al.*, Washington APS Meeting, April 1994; P. Baird, NATO Summer Institute July 18-30 (1994).

[53] W.R. Johnson, private communication.

[54] C.E. Wieman, private communication.

[55] L.A. Orosco, private communication.

[56] D. Budker, D. DeMille, E.D. Commins, and M.S. Zolotorev, *Phys. Rev. Lett.* **70**, 3019 (1993).

[57] CDF Collaboration: Young-Kee Kim, Presented at the Electroweak Session of the XXIXth Rencontres de Moriond, Meribel, France, March 12-19, 1994. FERMILAB-Conf-94/169-E, 1994.

[58] DØ Collaboration: Chang-Kee Jung, Presented at *The 27th Inter. Conf. on High Energy Physics*, Glasgow, July, 1994.

[59] J. Alitti *et al.*, (UA2 Collaboration), *Phys. Lett. B* **276**, 354 (1992).

[60] F. Abe *et al.*, (CDF Collaboration), *Phys. Rev. Lett.* **65**, 2243 (1990).

[61] M. Demarteau *et al.*, *Combining W Mass Measurements*, CDF/PHYS/CDF/PUBLIC/2552 and D0NOTE 2115.

[62] Young-Kee Kim, CDF Collaboration, Private Communication.

[63] J. Bijnens et al, LEP 200 Study, Aachen, 1986.

[64] C. Wyss, private communication.

[65] Akiya Miyamoto, Physics and Experiments with Linear e^+e^- Colliders, Hawaii, 1993, pp 141-165, edited by F.A.Harris, S.L.Olsen, S.Pakvasa, X. Tata, World Scientific, 1993.

[66] D. Wood, presented at *Physics in Collision 1994*, Tallahassee, FL, June 15-17, 1994.

[67] F. Abe *et al.*, *Phys. Rev. Lett.* **73**, 220 (1994);
F. Abe *et al.*, *Phys. Rev. Lett.* **69**, 28 (1992);
F. Abe *et al.*, *Phys. Rev. Lett.* **64**, 152 (1990);
J. Alitti *et al.*, *Phys. Lett. B* **276**, 365 (1992);
C. Albajar *et al.*, *Phys. Lett. B* **253**, 503 (1991).

[68] CDF Collaboration, paper submitted by W. Badgett to IX Topical conference on $p\bar{p}$ Physics, Tsukuba, Japan, October 1993; DØ Collaboration, presented by N.A. Graf at the same conference.

[69] J. Rosner, M.P. Worah, and T. Takeuchi, *Phys. Rev. D* **49**, 1363 (1994).

[70] F. Abe, *et al.*, *A Direct Measurement of the W Boson Width , (W))*, CDF/ANAL/ ELECTROWEAK/CDFR/2642, September 1994; submitted to *Phys. Rev. Lett.*

[71] DØ Collaboration: P. Grannis, presented at *The 27th Int. Conf. on High Energy Physics, Glasgow*, July,1994.

[72] DØ Collaboration: S.Abachi *et al.*, *Phys. Rev. Lett.* **72**, 2138 (1994).

[73] E.Laenen, J.Smith and W. van Neerven, *Phys. Lett. B* **321**, 254 (1994).

[74] CDF Collaboration: H.H. Williams, presented at *The 27th Int. Conf. on High Energy Physics, Glasgow*, July,1994.

[75] DØ Top Mass Fitting Group:Private Communication.

[76] DØ Collaboration: M. Strovink,European Physical Society Conference, Marseille, 1994.

[77] ATLAS Letter of Intent, CERN/LHCC/92-4, October 1992.

[78] CMS Letter of intent, CERN/LHCC/92-3, October 1992.

[79] ATLAS Internal Note, A.Mekki and L.Fayard, PHYS-NO-028,1993

[80] ATLAS Internal Note, Nicholas Andell, PHYS-NO-037, 1994.

[81] P. Igo-Kemenes, Physics and Experiments with Linear e^+e^- Colliders, Hawaii, 1993, pp 95-121, edited by F.A.Harris, S.L.Olsen, S.Pakvasa, X. Tata, World Scientific, 1993.

[82] Johann H. Kuhn, Physics and Experiments with Linear e^+e^- Colliders, Hawaii, 1993, pp 95-121, edited by F.A.Harris, S.L.Olsen, S.Pakvasa, X. Tata, World Scientific, 1993.

[83] D.Amidei, D.Baden, C. Hill, B.Klima, S.Parke, Top Quark Factory, 1994, unpublished.

[84] A workshop concerning top physics and Tevatron upgrades was held at the University of Michigan in November 1994. Working groups were formed, and a report is expected in summer 1995.

[85] G. Kane, C.P. Yuan, G. Ladinsky, *Phys. Rev. D* **45**, 124 (1992).

[86] D. Amidei and D.Winn, CDF Internal Note 2914, Sept 9, 1994.

[87] C.P. Yuan, *Strategies for Probing CP Properties in the Top Quark System*, MSUHEP-50123, January 1995; G. Grzadkowski and J. Gunion, *Phys. Lett. B* **287**, 237 (1992).

[88] C.P. Yuan, *Phys. Rev. D* **41**, 42 (1990); D.O. Carlson and C.P. Yuan, *Phys. Lett. B* **306**, 386 (1993).

[89] R.K. Ellis and S. Parke, *Phys. Rev. D* **46**, 3785 (1992).

[90] D. Gerdes, CDF Internal Note 2865.

[91] K. Fujii, T. Matsui, Y. Sumino, *Phys. Rev. D* **50**, 4341 (1994).

[92] D. Schaile, "Tests of the Electroweak Theory at LEP," CERN-PPE/93-213, December 1993.

[93] M.V. Terent'ev, *Yad. Fiz.* **18**, 870 (1973) [translation: *Sov. J. Nucl. Phys.* **18**, 449 (1974)].

[94] W.J. Marciano and A. Sirlin, *Phys. Rev. Lett.* **36**, 1425 (1976); *ibid.* **71**, 3629 (1993).

[95] D.I. Britton, *et al.*, *Phys. Rev. Lett.* **68**, 3000 (1992); C. Czapek *et al.*, *Phys. Rev. Lett.* **70**, 17 (1993).

[96] D. Bryman, *Comments Nucl. Part. Phys.* **21**, 101 (1993); W.J. Marciano, "e-μ-τ Universality", Cornell University Seminar, November 1993.

[97] S.Bethke, Proceedings of the Linear Collider Workshop in Waikoloa/Hawaii, April 1993;
S. Catani, presented at the International Europhysics Conference, Marseille, France, 22nd - 28th July 1993;
S. Banerjee, α_s *Measurements from Event Shape Variables using Z Data*, presented at the EPS Conference on High Energy Physics, Marseille, July 22-28, 1993, L3 Note 1460.

[98] The program EW-BHM (G. Burgers, W. Hollik, M. Martinez) was used for the contours in Figures 5, 6, 7, 8, 9, and 10 of this report. The program is described in CERN PPE 93-157.

[99] J. Ellis, G.L. Fogli, and E. Lisi, CERN TH-7261/94.

[100] D. Bardin *et al.*, LEP Electroweak Working Group Report, document in preparation.

[101] F. Richard, LAL-94-50, September 1994 (talk presented at the 27th International Conference on High Energy Physics, Glasgow, Scotland, 10-27 July 1994.

[102] P. Janot, Proceedings of the XXVIIth Rencontre de Moriond (*1992 Electroweak Interactions and Unified Theories*, edited by J. Tran Thanh Van), 1992, p. 317.

[103] A.Stange, W.Marciano, and S.Willenbrock, BNL-60340, ILL-(TH)-94-8, 1994.

[104] S.Mrenna and G.L.Kane, UM-TH-94-24, 1994.

[105] D. Chao, presented at Albuquerque DPF.

[106] For recent studies, see P. Grosse-Wiesemann, D. Haidt, and H.J. Schreiber, in *Workshop on e^+e^- Collisions at 500 GeV: the Physics Potential*, Munich, February; Annecy, June; Hamburg, September 1991, ed. P.M. Zerwas, DESY 92-123A (1992), p. 37; P. Janot, *ibid.*, p. 107; A. Djouadi, D. Haidt, B.A. Kniehl, B. Mele, and P.M. Zerwas, *ibid.*, p. 11, and references therein; J.F. Gunion, in *Physics and Experiments with Linear e^+e^- Colliders*, Hawaii, 1993, p. 166; P. Janot, *ibid.*, p. 192; and references therein.

[107] M.D. Hildreth, T.L. Barklow, and D.L. Burke, *Phys. Rev. D* **49**, 3441 (1994).

[108] Dieter Zeppenfeld, Physics and Experiments with Linear e^+e^- Colliders, Hawaii, 1993, pp 695-703, edited by F.A.Harris, S.L.Olsen, S.Pakvasa, X. Tata, World Scientific, 1993.

[109] CDF: F.Abe *et al.*, FERMILAB-Conf-94/158-E, 1994; DØ:A.Spadafora, FERMILAB-Conf-94/016-E, 1994.

[110] F. Abe *et al.*, (CDF Collaboration), contributed paper to the 27th International Cponverence on High Energy Physics, Glasgow, Scotland, July 20-27, 1994, FERMILAB-Conf-94/158-E (June 1994); A. Spadafora (DØ Collaboration), FERMILAB-Conf-94/016-E (January 1994).